

## RESEARCH ARTICLE

# Projecting ocean acidification impacts for the Gulf of Maine to 2050: New tools and expectations

Siedlecki, SA<sup>1\*</sup>, Salisbury, J<sup>2</sup>, Gledhill, DK<sup>3</sup>, Bastidas, C<sup>4</sup>, Meseck, S<sup>5</sup>, McGarry, K<sup>1</sup>, Hunt, CW<sup>2</sup>, Alexander, M<sup>6</sup>, Lavoie, D<sup>7</sup>, Wang, ZA<sup>8</sup>, Scott, J<sup>6</sup>, Brady, DC<sup>9</sup>, Misna, I<sup>10</sup>, Azetsu-Scott, K<sup>11</sup>, Liberti, CM<sup>9</sup>, Melrose, DC<sup>12</sup>, White, MM<sup>13</sup>, Pershing, A<sup>14</sup>, Vandemark, D<sup>2</sup>, Townsend, DW<sup>9</sup>, Chen, C<sup>15</sup>, Mook, W<sup>13</sup>, and Morrison, R<sup>16</sup>

Ocean acidification (OA) is increasing predictably in the global ocean as rising levels of atmospheric carbon dioxide lead to higher oceanic concentrations of inorganic carbon. The Gulf of Maine (GOM) is a seasonally varying region of confluence for many processes that further affect the carbonate system including freshwater influences and high productivity, particularly near the coast where local processes impart a strong influence. Two main regions within the GOM currently experience carbonate conditions that are suboptimal for many organisms—the nearshore and subsurface deep shelf. OA trends over the past 15 years have been masked in the GOM by recent warming and changes to the regional circulation that locally supply more Gulf Stream waters. The region is home to many commercially important shellfish that are vulnerable to OA conditions, as well as to the human populations whose dependence on shellfish species in the fishery has continued to increase over the past decade. Through a review of the sensitivity of the regional marine ecosystem inhabitants, we identified a critical threshold of 1.5 for the aragonite saturation state ( $\Omega_a$ ). A combination of regional high-resolution simulations that include coastal processes were used to project OA conditions for the GOM into 2050. By 2050, the  $\Omega_a$  declines everywhere in the GOM with most pronounced impacts near the coast, in subsurface waters, and associated with freshening. Under the RCP 8.5 projected climate scenario, the entire GOM will experience conditions below the critical  $\Omega_a$  threshold of 1.5 for most of the year by 2050. Despite these declines, the projected warming in the GOM imparts a partial compensatory effect to  $\Omega_a$  by elevating saturation states considerably above what would result from acidification alone and preserving some important fisheries locations, including much of Georges Bank, above the critical threshold.

**Keywords:** Ocean acidification, Gulf of Maine, Projection, Regional simulations, Species sensitivity, Warming

## Introduction

Ocean acidification (OA) is increasing predictably in the global ocean as rising levels of atmospheric carbon dioxide ( $\text{CO}_2$ ) are absorbed by the ocean air–sea interface, resulting in higher oceanic inorganic carbon concentrations (Gattuso et al., 2015; Le Quéré et al., 2018;

Friedlingstein et al., 2019). Over time, ocean uptake of  $\text{CO}_2$  perturbs the entire carbonate system, with a concomitant reduction in surface pH, carbonate ion ( $\text{CO}_3^{2-}$ ), and carbonate saturations states (here, we focus on aragonite saturation state or  $\Omega_a$ ; Bates et al., 2014). Since the beginning of the 19th century, the pH of the world's surface

<sup>1</sup>Department of Marine Sciences, University of Connecticut, Groton, CT, USA

<sup>2</sup>Ocean Process Analysis Laboratory, University of New Hampshire, Durham, NH, USA

<sup>3</sup>NOAA OAR Ocean Acidification Program (OAP), Silver Spring, MD, USA

<sup>4</sup>Massachusetts Institute of Technology, Sea Grant Program, Cambridge, MA, USA

<sup>5</sup>NOAA, Milford Laboratory, Milford, CT, USA

<sup>6</sup>NOAA Physical Sciences Laboratory, Boulder, CO, USA

<sup>7</sup>Fisheries and Oceans Canada, Maurice Lamontagne Institute, Quebec, Canada

<sup>8</sup>Woods Hole Oceanographic Institution, Woods Hole, MA, USA

<sup>9</sup>University of Maine, Orono, ME, USA

<sup>10</sup>Environmental Protection Agency Region 1, Boston, MA, USA

<sup>11</sup>Fisheries and Oceans Canada, Bedford Institute of Oceanography, Nova Scotia, Canada

<sup>12</sup>NOAA, Narragansett Laboratory, Narragansett, RI, USA

<sup>13</sup>Mook Sea Farm, Walpole, ME, USA

<sup>14</sup>Gulf of Maine Research Institute, Portland, ME, USA

<sup>15</sup>University of Massachusetts, Dartmouth, MA, USA

<sup>16</sup>Northeastern Regional Association of Coastal Ocean Observing Systems, Portsmouth, NH, USA

\*Corresponding author:  
Email: [samantha.siedlecki@uconn.edu](mailto:samantha.siedlecki@uconn.edu)

ocean has decreased by 0.1 units (Caldeira and Wickett, 2003; Orr et al., 2005; Doney et al., 2009), and further pH reductions on the order of 0.2–0.3 units are predicted by 2100 under Intergovernmental Panel on Climate Change (IPCC) AR2 scenarios (Feely et al., 2009) due to the projected increase in atmospheric CO<sub>2</sub>.

The carbonate system in coastal waters is impacted not only by changes in atmospheric CO<sub>2</sub> concentrations but also by varying fluxes of dissolved inorganic carbon (DIC), total alkalinity (TA), and nutrients derived from local and remote processes. In the Northwest Atlantic, local processes include low alkalinity river discharge (Salisbury et al., 2008), atmospheric deposition of acidic and alkaline compounds (Doney et al., 2007), sedimentary processes (Fennel et al., 2008), and coastal eutrophication (Wallace et al., 2014; Rheuban et al., 2019). Therefore, the Gulf of Maine (GOM) is a region of confluence for many processes that further affect the carbonate system. Two main regions within the GOM currently experience suboptimal carbonate conditions for many marine organisms (i.e.,  $\Omega_a < 1.5$ )—the nearshore and subsurface deep shelf. In nearshore regions, close to the coastline and less than 50 m in water depth, for example, five large rivers discharge into the GOM and mix with more saline waters in part due to the large tides. In addition, acidic and alkaline compounds from many of the coal-fired power plants upwind of the GOM are deposited in the surface waters (Doney et al., 2007) and watershed, and there is a south-to-north decreasing gradient in both human population density and eutrophication. The interannual to decadal variability of large-scale, more remote circulation patterns, like the Gulf Stream, Labrador Current, and Atlantic meridional overturning circulation, delivers warmer, saltier waters from the south or cooler fresher waters from the north, all of which contribute to temporal and spatial variability in the carbonate chemistry of the GOM. Seasonal variation in the delivery of locally produced and imported organic materials to subsurface deeper shelf offshore regions (beyond 50-m isobaths) contributes to the variability in biologically suboptimal conditions, which may be further influenced by sedimentary processes (Wang et al., 2017). Regional studies over the last decade have identified that these drivers of acidification in the GOM (summarized in the 2015 Maine OA Study Commission; Salisbury et al., 2008; Wang et al., 2013; Strong et al., 2014; Gledhill et al., 2015; State of Maine Legislature, 2015; Salisbury et al., 2018), the relative contributions of each driver, and in particular the mixing of water masses, remain poorly understood.

Sutton et al. (2016) performed an analysis of GOM data using the Pacific Marine Environmental Laboratory (PMEL)/University of New Hampshire (UNH) Coastal CO<sub>2</sub> Buoy D (43.02°N, 70.54°E, “Buoy D”) among other moorings and, after adopting assumptions about past atmospheric CO<sub>2</sub> values, concluded that  $\Omega_a$  had never dropped below 1.6 in the GOM during preindustrial times. That study also showed that during the period 2010–2013, coastal GOM waters at Buoy D regularly and persistently dipped below the preindustrial minima of  $\Omega_a$  and pH. This historical view and the observed impacts on

mollusk larvae (e.g., Salisbury et al., 2008; Waldbusser and Salisbury, 2014; Ekstrom et al., 2015; Waldbusser et al., 2015) informed our choice of the critical  $\Omega_a$  threshold of 1.5 in this study. The surface waters of the GOM at Buoy D recently experienced conditions below that threshold 9% of the year using the Buoy D record spanning 2010–2020, with peak exposure to low  $\Omega_a$  in the winter months (December–March; **Figure 1**). Nearshore, at the University of New Hampshire Coastal Marine Lab (UNH CML) station (43.07°N, 70.71°E), conditions existed below the  $\Omega_a$  threshold of 1.5 in the surface waters (**Figure 1**) 41% of the time over that same time period. The nearshore CML location experiences more freshwater influence than Buoy D, which is about 18 km offshore (**Figure 2**), and freshwater has a low  $\Omega_a$  in this area due to the low alkalinity content of local rivers (Hunt et al., 2011). Despite the existence of some oyster growers upstream, the area around the CML location was not an area of prominent shellfish harvest over the observation period presented here (2010–2019).

The history of direct high-quality carbonate chemistry observations in the GOM is relatively short, and each observational program provided for limited spatial and mostly surface water coverage. The deployment of “Buoy D” equipped with an MAPCO2 system (Sutton et al., 2019) was one of the earliest observational efforts in the region. In addition to this system, in 2004, UNH researchers began monthly-to-seasonal transects in the Western GOM, from shore to Wilkinson Basin (WB), making discrete measurements of TA and DIC at various depths, as well as partial pressure of CO<sub>2</sub> (pCO<sub>2</sub>) in surface water. Regular, GOM-wide, dedicated research cruises conducting near-synoptic inorganic carbon sampling of the full water column along select transects did not begin until 2007. Since then, these surveys have been repeated every 3–4 years and are supplemented by annual seasonal surveys performed as part of the NOAA National Marine Fisheries Service Ecosystem Monitoring surveys and by individual studies (e.g., Wang et al., 2017). Today, the observational network has expanded and includes many subsurface observations (**Figure 2**) and community science-based sampling events like “Shell Day” (Rheuban et al., 2021; **Figure 2**). Such direct observations have indicated that the least buffered waters on the east coast of the United States reside on the Northwest Atlantic shelves, which may make them exceptionally susceptible to acidification (Wang et al., 2013).

In an effort to extend the observational record back several decades, Salisbury and Jönsson (2018) used surface temperature and salinity outputs of a general circulation model applied to empirical algorithms trained from the Surface Ocean CO<sub>2(aq)</sub> Atlas (Bakker et al., 2016) and informed by satellite chlorophyll to derive the estimates of past OA conditions in the GOM. The analysis of a 34-year reconstructed record (1981–2014) revealed decades when the carbonate system was perturbed to an extent greater than expected solely from atmospheric uptake of CO<sub>2</sub>. In fact, recent temperature and salinity changes in the GOM (between 2005 and 2014) appear to have partially compensated for the effects of OA over the past

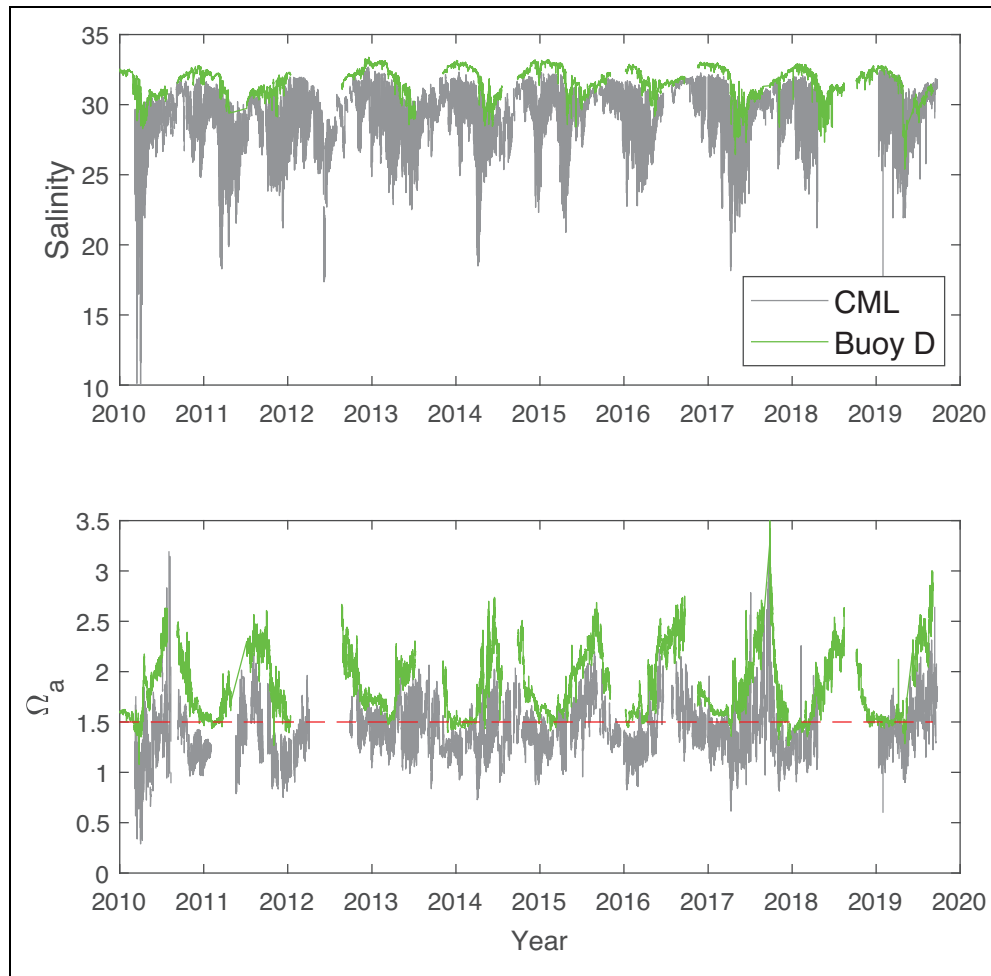
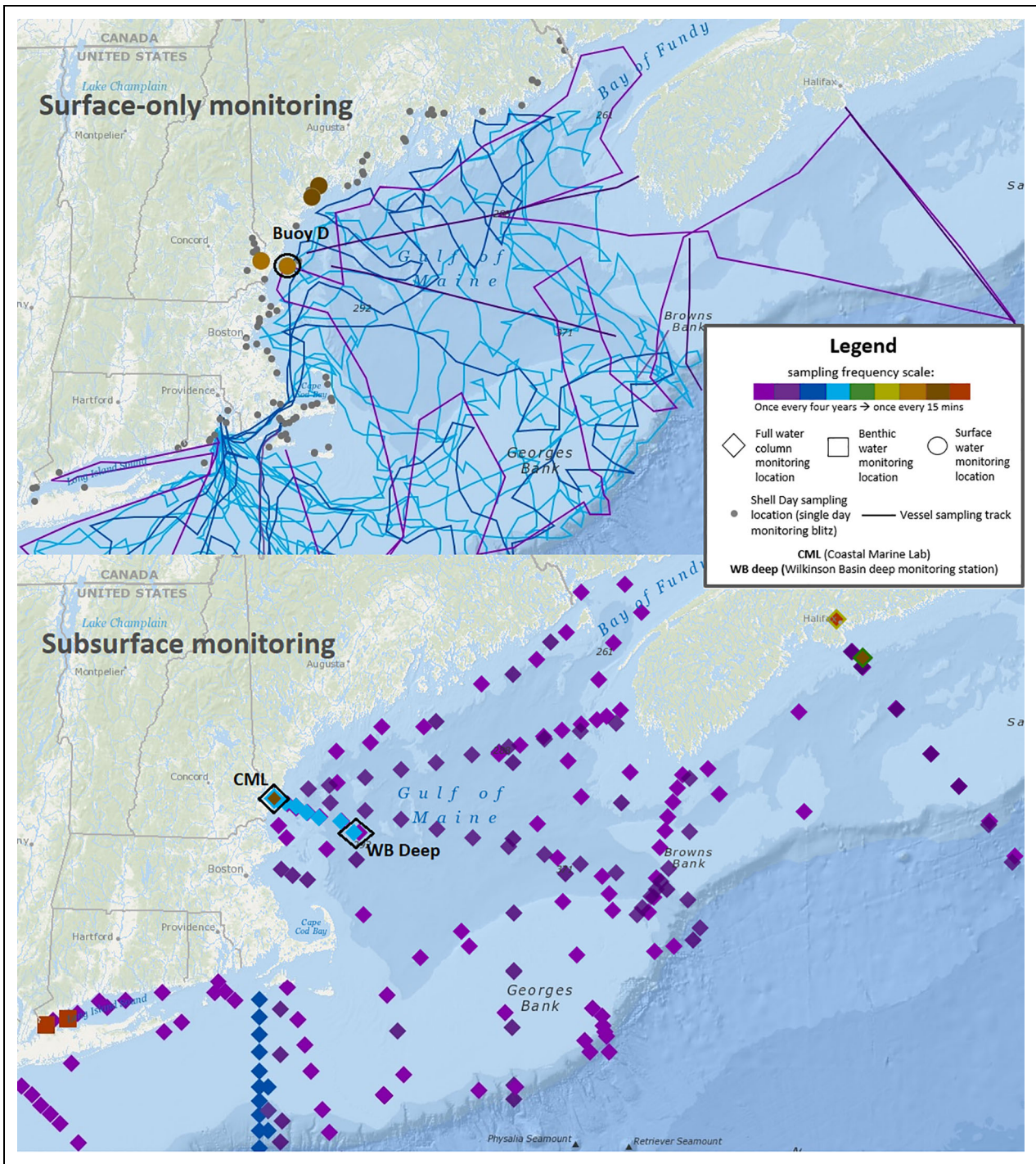


**Figure 1.** Surface  $\Omega_a$  variability nearshore and midshelf in the Gulf of Maine. Hourly salinity (top) and aragonite saturation state ( $\Omega_a$ , bottom) measured at the University of New Hampshire Coastal Marine Lab (CML, gray line; 43.07°N, 70.71°E) and the Pacific Marine Environmental Laboratory/University of New Hampshire Coastal CO<sub>2</sub> Buoy D (green line; 43.02°N, 70.54°E). The  $\Omega_a$  values were calculated from in situ measurements of salinity, water temperature, partial pressure of carbon dioxide ( $p\text{CO}_2$ ), and total alkalinity modeled from salinity and water temperature using an empirical model (McGarry et al., 2021). The red dashed line in the lower panel represents the threshold of 1.5. Calculations were performed using the CO<sub>2</sub>SYST program (van Heuven et al., 2011) with the  $K_1$  and  $K_2$  constants of Millero (2010), the  $K_{\text{SO}_4}$  of Dickson (1990a, 1990b), and  $K_B$  of Uppstrom (1974). The variability at the CML location exceeds that at the Buoy D location approximately 11 km further offshore. The conditions at CML are also more severe. Both of these observations are consistent with the increased presence of freshwater at CML (upper panel), which in this region is known to be suboptimal for marine organisms. DOI: <https://doi.org/10.1525/elementa.2020.00062.f1>

decade by causing an increase in  $\Omega_{\text{arag}}$  of 0.4 in surface waters. The analysis also revealed markedly different behavior between pH and  $\Omega_{\text{ar}}$ . The pH was found to decline at a rate of  $-0.018 \text{ decade}^{-1}$ , driven primarily by OA and was largely in agreement with global surface water rates of decline over the past 30 years of  $-0.0013$  to  $-0.0025$  per year (Bates et al., 2014). The OA effect on  $\Omega_a$ , on the other hand, is partially obscured by increased temperature and buffering by higher salinity waters entering the GOM (Salisbury and Jönsson, 2018). The differing responses of individual carbon variables, such as pH and  $\Omega_{\text{ar}}$ , to changes in temperature and salinity can lead to varying seasonal amplification or attenuation in these variables globally, which can also impact trends (Kwiatkowski and Orr, 2018; Jiang et al., 2019). Using this

reconstructed time series, Salisbury and Jönsson (2018) estimated the “time of emergence” or the time required for the atmospheric CO<sub>2</sub> signal to emerge from background natural variability. They found that observing a discernible OA signal in pH may require 30 years of sustained measurements and up to a century to observe the OA signal in  $\Omega_{\text{arag}}$  (Salisbury and Jönsson, 2018). Despite these long emergence times, nearshore and offshore GOM regions influenced by local rainfall, freshwater, and respiration are already experiencing event-scale reductions in  $\Omega_a$  considered suboptimal for many marine organisms.

In the future, OA is projected to cause global annual economic losses up to US\$100 billion due to decreased shellfish production, based on the use of the highest CO<sub>2</sub> emission scenarios for 2100 (in this case scenario A1B) by



Downloaded from <http://online.ucpress.edu/elementa/article-pdf/9/1/00062/462357/elementa.2020.00062.pdf> by guest on 07 June 2021

**Figure 2.** Map of existing carbonate system observations in the Gulf of Maine. Existing capacity for monitoring ocean acidification through carbonate system observations in the Gulf of Maine and New England region for surface (upper panel) and subsurface (lower panel) waters, updated from Gledhill et al. (2015). Carbonate system monitoring by buoys and vessels, as well as approximate cruise tracks and sampling waypoints, is color coded according to the frequency of occupation. “Shell Day” (August 2019) monitoring locations represent a single-day monitoring blitz and are therefore color coded gray (Rheuban et al., 2021). See Table S3 for observations depicted including parameters measured, sampling frequency, depth, and projects. DOI: <https://doi.org/10.1525/elementa.2020.00062.f2>

the IPCC to drive spatially coarse resolution global models (Narita et al., 2012). Although oceanographic, social, and economic variability all dictate that the impacts of OA will not be uniform, New England is increasingly dependent on shellfisheries (Figure S1; Gledhill et al., 2015). Large-scale and regional studies show that the combination of

global and local drivers of acidification of the waters off New England makes its shellfisheries, both the predominantly offshore wild harvest fisheries and predominantly nearshore aquacultural production, potentially among the most vulnerable to OA in the United States (Ekstrom et al., 2015, Gledhill et al., 2015), with socioeconomic

consequences for the communities that rely on these industries. This vulnerability to OA also has implications for the shellfisheries and shellfish-dependent communities of Atlantic Canada. Regional economic and vulnerability analyses, focused on the scallop industry and scallop landings in Massachusetts, found that OA is projected to threaten tens of thousands of jobs and cause hundreds of millions of dollars in losses during the 21st century (Cooley and Doney, 2009; Cooley et al., 2015; Ekstrom et al., 2015; Rheuban et al., 2018).

Global projections with spatial resolution of a degree or more, relied upon by the IPCC, cannot resolve coastal processes with complex feedbacks known to be important to the regional evolution of the OA signal. Some high-resolution global projections have been developed which perform well in some coastal settings (Saba et al., 2016; Alexander et al., 2020) but lack regional biogeochemical processes which can amplify or dampen these global changes, particularly in coastal shelf regions like the GOM.

Here, we use a combination of regional high-resolution simulations that include coastal processes to project OA conditions for the GOM in 2050 and consider what this projection portends for its ecosystems with a particular focus on the nearshore and subsurface environments. First, we review the science specific to acidification of coastal waters (nearshore to shelf break) extending from the Canadian Scotian Shelf southward to the northern reaches of the Mid-Atlantic Bight. Next, we review what is known about the sensitivity of the regional ecosystem inhabitants with a focus on those of socioeconomic value to the region. We then describe the methods employed to compute trends and provide a suite of regional projections. Finally, we discuss the results of the projections and their implications for GOM ecosystems.

### **Background relevant to OA in the GOM**

The GOM is a productive temperate continental shelf sea bounded by Cape Cod to the west, Georges Bank to the south, and Nova Scotia to the northeast. It is well known for its large semidiurnal tides and their resulting impact on mixing and also for the high commercial value of its fish and shellfish landings. It is separated from the open northwest Atlantic by both Georges and Browns banks. Considerable control on seasonal to interannual circulation patterns is exerted via shelf–sea exchange through the narrow northeast channel (NEC), which separates Georges and Browns banks and by the fresher coastal source waters from along the Scotian Shelf (Townsend, 1991; Pringle, 2006). The GOM has an average tidal range > 3.0 m and experiences large seasonal amplitudes in surface salinity (Geyer et al., 2004), net primary productivity (O'Reilly et al., 1987), sea surface temperature (SST) and  $p\text{CO}_2$  (Vandemark et al., 2011). The key circulation feature influencing the region is the Maine Coastal Current, which flows counterclockwise and delivers freshwater and constituents from the northeast GOM to the southwest GOM (Pettigrew et al., 2005).

Physical processes that deliver and mix the nutrient pools supporting the GOM ecosystem (e.g., strong tides, wind-driven mixing, large annual ranges in temperature

and salinity) also generate thermodynamic variability in carbonate system parameters at diurnal through annual scales. Further, such processes contribute to an intense annual cycle of  $\text{CO}_2$ , whereby disequilibrium with the atmosphere is partially balanced by an air–sea flux of  $\text{CO}_2$  (Shadwick et al., 2011; Vandemark et al., 2011; Wang et al., 2017). The degree to which physical variability can modify OA in the GOM is substantial (Salisbury and Jönsson, 2018). In a climatological study using data from 1950 to 2013, the GOM recorded an intraannual SST range of  $5\text{ }^\circ\text{C}$ – $15.5\text{ }^\circ\text{C}$  and salinity range of 31.5–32.5 (Richaud et al., 2016). The annual temperature range alone elicits a significant change in the carbonate system. For example, assuming the approximate mean GOM salinity (32.2), the mean TA ( $2,184\text{ }\mu\text{mol kg}^{-1}$ ) and an atmospherically equilibrated seawater surface  $p\text{CO}_2$  (400 uatm), temperature variability causes an annual increase of 0.013 in  $\text{pH}_{\text{TOT}}$  (pH total scale) and 1.06 in  $\Omega_a$ .

Within the GOM, the period spanning 2003–present (the period for which moored data exist via the Northeast Regional Association of Coastal Ocean Observing Systems) has been characterized by temporally coherent oceanographic phases that last on the order of 1–3 years. These phases result from periods of primarily warm slope-water intrusions into deeper layers of the GOM, bringing warm and salty high-nutrient waters, followed by episodes of increased shelf-water fluxes from the Scotian Shelf that bring colder and fresher low-nutrient waters to the GOM (e.g., Townsend et al., 2014, 2015). Beginning in about 2008, the GOM entered an extended warm and salty phase, which was an important contributor to the anomalously warm surface waters reported by Pershing et al. (2015). However, in the last 7 years, since 2013, greater short-term variability has been observed, with some of the coldest (and freshest) and warmest (and saltiest) episodes in the more than 15-year moored record. The timing of these water mass fluxes and associated surface temperature changes maintained by atmospheric heat flux (Chen et al., 2014, 2018) have combined to produce short-term, rapid warming of surface waters in the Gulf (on the order of  $0.15\text{ }^\circ\text{C y}^{-1}$ ) as reported by Pershing et al. (2015). Such water mass fluctuations may be related to changes in the Labrador Current (Townsend et al., 2010, 2015; Mountain, 2012; Claret et al., 2018) and a northerly shift of the Gulf Stream as described in Saba et al. (2016; also see Grodsky et al., 2017). Although the majority of the warming trend over the period 1982–2018 can be attributed to natural variability, a third of the trend has been attributed to anthropogenic warming (Chen et al., 2020).

Seasonal variability in the carbonate system of the water column in the GOM is affected mostly by and synchronized largely with the seasonal progression of stratification overturn, primary production, respiration–remineralization, and water mixing (Wang et al., 2017). Different processes may alternate to exert the main control on the variability at certain times of the year (Wang et al., 2017). In the winter, saturation states at the surface are at their lowest (**Figure 1**) and the water column is well mixed. Subsequently, spring blooms draw down carbon at the surface subsequently raising the  $\Omega_a$ , while at the same

time, the freshet arrives bringing stratification and low  $\Omega_a$  waters to the surface. Over the summer, surface waters warm and stratification continues to isolate the bottom waters, while circulation changes act to retain local organic material in subsurface waters where remineralization of that material draws down saturation states. The fall brings increased storms, precipitation, mixing, and a decline in saturation states near the surface as seasonal trends cool the surface and reduce productivity. Overall, photosynthesis–respiration is the main driver controlling the seasonal variability of  $\Omega_a$  (Wang et al., 2017). Less is known about subsurface seasonal patterns. Interannual variability in the system is primarily governed by the magnitude of ocean productivity and by the relative supply of differing water sources from regional currents. Waters sourced from the Labrador Current and Gulf of St. Lawrence have lower carbonate ion concentrations (and thus lower  $\Omega_a$ ) versus those supplied by the higher salinity Gulf Stream. Within the GOM, these waters are subsequently modified by remineralization and respiration as well as riverine inputs (Wanninkhof et al., 2015; Wang et al., 2017).

#### **Sensitivity of GOM fauna to OA**

Many marine species are likely to be affected by projected OA conditions in 2050. Evidence supporting the effects of OA on commercially important marine bivalves is clear (Gazeau et al., 2013; Waldbusser and Salisbury, 2014), and more information continuously becomes available for other groups such as crustaceans and fish (e.g., Dixon et al., 2010; Keppel et al., 2012; Long et al., 2016a; Rodriguez-Dominguez et al., 2018). These data indicate that acute or chronic responses are observed between  $\Omega_a$  of 1.0 and 2.0. The response is species-dependent, but  $\Omega_a = 1.5$  is a conservative estimate of when physiological effects have been observed and as such will be referred to as suboptimal conditions for marine organisms (i.e.,  $\Omega_a < 1.5$ ). The physiological effects of OA on life stages and populations of particular species are typically better understood than the ecological consequences at ecosystem levels. Similarly, the short-term effects of  $\Omega_a$ , pH, and buffering capacity on marine organisms have been better characterized than their long-term effects. Thus, a unified understanding of long-term combined effects of OA with accompanying changes in temperature, circulation patterns, freshwater inputs, and productivity, among other factors that are also projected to change in the region, is still lacking.

In the GOM, there has been progress in understanding the effects of carbonate chemistry in key fisheries and aquaculture industries, such as those that target the American lobster, Eastern oyster, and Atlantic sea scallop (reviewed by Gledhill et al., 2015). However, this progress falls short when considering the number of shell-forming species with high and very high climate vulnerability on the Northeast U.S. continental shelf (Hare et al., 2016), their complex life cycles, and the interactions of environmental factors. Table 1 of Gledhill et al. (2015) summarizes the acidification studies of seven commercially important species of the New England/Nova Scotia region, including the American lobster, four species of

bivalves, the summer flounder, and the Atlantic longfin squid. Studies on approximately 140 additional species living in or related to species living in the region are also available (Table S1 in Gledhill et al., 2015). Here, we included more than 60 studies, conducted with species from the GOM since 2015 and focused on commercially important species (Tables S1 and S2). Below, we discuss the highlights from these recent studies in the context of prior results discussed in previous efforts (e.g., Gledhill et al., 2015; Hare et al. 2016).

Fisheries in the GOM rendered over US\$1.2 billion in 2017 in the United States alone, with 74% of the total landings composed of crustaceans and bivalves. These two groups have been identified as highly susceptible to OA and temperature increases, and both have complicated life histories with their larval stages primarily pelagic and adult stages mostly benthic. American lobster is currently the highest value fishery in the United States and Canada and the top species landed by weight and revenue in the region, with US\$551 million harvested from the U.S. GOM in 2017 (NOAA Fisheries, 2019), 1.42 billion CDN in Atlantic Canada in 2018, with New Brunswick and Nova Scotia contributing a landed value of 1.06 billion CDN, of which US\$730 million were harvested from Nova Scotia (Department of Fisheries and Oceans, 2018, Zonal Interchange File [database], Ottawa, accessed August 4, 2020). Although American lobsters have been observed in waters as deep as 800 m, the majority of landings occur from waters shallower than 80 m in the GOM (Tanaka and Chen, 2016; Oppenheim et al., 2019). Warming effects in lobsters have been studied extensively (e.g., Rheuban et al., 2017; Jaini et al., 2018; Boavida-Portugal et al., 2018). In Table S1, we included recent studies examining the effects of OA alone or both OA and warming in different life stages, often at experimental  $\text{CO}_2$  levels higher than projected for 2050. Larval studies up to Stage IV of development found that warming had a greater adverse effect than increased  $\text{pCO}_2$  alone (Waller et al., 2017) and when combined, increased temperature and  $\text{pCO}_2$  altered dry mass, carapace length, swimming speed, feeding rates, and survival of lobsters. On the other hand, experiments with older larvae (Stage V) to juveniles found increases in mortality, slower development, and increases in aerobic capacity under increased  $\text{pCO}_2$  alone (Menu-Courey et al., 2019). Similarly, McLean et al. (2018) found that increasing  $\text{pCO}_2$  resulted in decreases in length and biomass, longer intermolting periods, and more susceptibility to shell disease in juvenile lobsters. Juvenile lobsters also showed immunosuppression and reduced cardiac performance when exposed to increased  $\text{pCO}_2$  and acute thermal stress for 60 days (Harrington and Hamlin, 2019). These recent studies further support detrimental physiological responses to increased OA for different life stages of the American lobster, which will be exacerbated by accompanying warming conditions.

In GOM, bivalves accounted for 36% of the total U.S. landings revenues in 2017, with the Atlantic sea scallop yielding US\$341 million (28%) followed by the eastern oyster yielding US\$35 million (3%). In Canada, the sea scallop fisheries for Nova Scotia and New Brunswick

combined yielded US\$164 million CDN, while eastern oyster aquaculture for the same regions yielded US\$20 million CDN (Statistics Canada, Table 32-10-0107-01 Aquaculture, production and value. Retrieved November 22, 2019). The majority of their adult benthic habitat occupies the nearshore and shallow shelf regions of the GOM, except for Atlantic sea scallops that reside further offshore with a regional hot spot around Georges Bank. Recent integrated assessment models for the Atlantic sea scallop (Cooley et al., 2015; Rheuban et al., 2018) suggest that under different CO<sub>2</sub> emission scenarios and different impact and management conditions, sea scallop biomass could be reduced between 13% and 50% by the end of the century (Table S1). These projections and the high revenue underscore an urgent need for laboratory and field research on how sea scallops respond to OA and increased water temperature, so that the industry and managers can respond accordingly to maintain sustainable stocks. Similarly, the Atlantic surfclam is another commercially prized species, with ample distribution from Canada's Gulf of St. Lawrence to North Carolina in the United States, that has already shifted northward in its distribution (Timbs et al., 2019), but studies of its response to OA have begun only recently (Pousse et al., 2020; Measek et al., 2021; Table S1).

In comparison with scallops and surfclams, eastern oysters are better studied, and their response to OA varies across life stages, with early stages typically being more susceptible than adults (Table S1). Other bivalve species such as soft-shell clams and mussels have also shown this pattern (Tables S1 and S2). Although there are more studies on early life stages, a few recent studies of the eastern oyster *Crassostrea virginica* have examined the short-term effects of OA on adults and found minimal change in length or in gaping behavior (Table S1). Both studies of adults in Table S1 involved experiments of relatively short duration, and calcite in adult shells has less corrosivity than aragonite in larval shells in general. Although gaping behavior in adult oysters did not seem affected, research on other adult bivalves, such as blue mussels, bay scallops, and hard clams, has shown detrimental effects with reduced growth rates and tissue weights when exposed to OA (Table S1). Less frequent field experiments also support adverse OA effects in bivalves as evidenced by reductions in settlement rates when low pH conditions prevail in sediments for *Mya arenaria* and *Nucula* spp (Table S1). An increased repertoire of studies, including more species, different life stages, multiple concurrent stressors, field and lab experiments, modeling projections, transgenerational observations (Griffith and Gobler, 2017), and potential for mitigation in multispecies studies (Young and Gobler, 2018), have considerably improved the understanding of potential responses to OA for individual bivalve species in the GOM.

Several studies from the region have also highlighted the complex response of finfish to OA (Tables S1 and S2). Atlantic sea herring (*Clupea harengus*) is an important commercial and keystone species at the base of the food web in marine ecosystems in the GOM. Studies on the effects of OA on swimming behavior, energetic costs, and

survivorship of this species have yielded contrasting results (Table S1). This variability suggests that different populations in the region might vary in their response to OA, which should be explored further (Leo et al., 2018). Similar to results from bivalve species above, studies on the forage fish Atlantic silverside (*Menidia menidia*) and inland silverside (*M. beryllina*) have highlighted differences between experiments where OA was a unique factor and experiments that included additional stressors such as high temperature (Table S2).

Experimental studies in the GOM have also illustrated contrasting responses of different physiological parameters within a life stage for a single species. For example, Stiasny et al. (2018) observed that cod larvae were larger under energy limitation in the elevated CO<sub>2</sub> treatment compared to the ambient CO<sub>2</sub> treatment, but larvae under elevated CO<sub>2</sub> had developmental impairments in critical organs, such as the liver. All these studies make clear that our capacity to replicate environmental and biological complexity in experimental studies is limited, yet more sophisticated and longer term studies are critical to enable further understanding of physiological mechanisms, energetic balances in organisms, and population dynamic consequences of OA in marine species. A handful of other studies, including responses through trophic webs (e.g., Jin et al., 2015) and other ecological interactions (e.g., Fay et al., 2017; Schulz et al., 2017; Gilbert, 2020; Raven et al., 2020; Tester et al., 2020; Wilson et al., 2020), have suggested potentially larger but varied ecological and ecosystem consequences of OA in the GOM. Thus, a better integration of our current knowledge, predictive capability, and collaboration will be key to addressing management and societal changes that ameliorate OA consequences in the region and preserve the sustainability of marine resources and the services they provide to the GOM.

### Methods for quantifying trends and projections of OA in the GOM

In this section, we describe the methods employed to compute regional trends from observations, the evaluation methods we relied on for the regional models of the area, and the approach we used for the entire suite of regional projections produced for this work. A combination of regional high-resolution simulations that include coastal processes was used to project OA conditions for the GOM into 2050. We also discuss the approach for each model and include some discussion of the global models as well.

### Observations and historical trend analysis

Several different data sets were used for this work including observations from Buoy D, the CML site, and some regional transects including those within WB. Surface observations from the moored NOAA PMEL/UNH Coastal CO<sub>2</sub> Buoy D, as described in Sutton et al. (2019), were used in this work. The Buoy D data set spans the period 2006–2018. The CML data set spans 2008–2019. Buoy temperature and salinity were measured by a Sea-Bird Electronics SBE-16plus (Sea-bird electronics, Bellevue WA, salinity and temperature accuracies of  $\pm 0.0005$  Siemens (S) m<sup>-1</sup> and  $\pm 0.005$  °C, respectively), while those

from CML were measured with an Aanderaa 4319B (Xylem, Rye Brook NY, salinity and temperature accuracies of  $\pm 0.0018 \text{ S m}^{-1}$  and  $\pm 0.05 \text{ }^\circ\text{C}$ , respectively). PMEL/UNH buoy  $\text{CO}_2$  measurements were from an MAPCO2 system (Sutton et al., 2019), while those from the CML site were made using a showerhead-type equilibrator with headspace air recirculated through a Li-cor LI840 nondispersive infrared detector (details of this system in Hunt et al., 2017, and references therein). Each  $\text{CO}_2$  system was calibrated with a  $\text{CO}_2$ -free gas stream and a  $\text{CO}_2$ /nitrogen mixture that was cross-calibrated to standard gases from NOAA/Earth System Research Laboratories. The uncertainty of the PMEL/UNH  $\text{CO}_2$  measurements was better than  $\pm 3 \text{ } \mu\text{atm}$ , while that of the CML  $\text{CO}_2$  measurements was estimated as  $\pm 3 \text{ } \mu\text{atm}$  (Vandemark et al., 2011). Calculations were performed using the CO2SYS program (van Heuven et al., 2011) with  $K_1$  and  $K_2$  constants from Millero (2010),  $\text{KSO}_4$  from Dickson (1990a, 1990b), and  $\text{KB}$  from Uppstrom (1974).  $\Omega_a$  at both the PMEL/UNH Coastal  $\text{CO}_2$  Buoy and UNH CML sites (**Figure 2**) was calculated from in situ measurements of salinity, water temperature,  $\text{pCO}_2$ , and TA modeled from salinity and water temperature using an empirical model (McGarry et al., 2021). CML monthly salinity and  $\Omega_a$  climatologies (**Figure 2**) were constructed from mean monthly values, which were interpolated to a daily time step (“pchip,” MATLAB, MathWorks Natick MA) and smoothed with a 60-day moving mean (“smooth,” MATLAB).

Monthly-to-seasonal cross-shore transects have been conducted by the University of New Hampshire since 2004. The transect line runs more than 80 km west to east, ending at station WB-7 (bottom depth approximately 250 m) in WB, one of the three deeper basins in the GOM (**Figure 2**). Discrete samples for lab analyses are collected from Niskin bottles closed at depth intervals through the water column.  $\Omega_a$  at the WB-7 site was calculated from in situ measurements of salinity and water temperature (from a SBE-16plus) and bottle measurements of DIC and TA. DIC of unfiltered water was measured using an Apollo SciTech AS-C2 analyzer (Newark DE), while TA of unfiltered water was measured via Gran titration using an Apollo SciTech AS-ALK2. DIC and TA method precisions were  $\pm 2 \text{ } \mu\text{mol kg}^{-1}$ . Further details of DIC and TA sample

collection and lab analysis methods can be found in Hunt et al. (2013).

The water column at WB-7 was divided into three depth strata for trend analysis, based on sampling consistency over the program period, with the aim to isolate the surface, mixed layer, and bottom conditions. Linear trend lines were calculated for each depth stratum by using deseasonalized data based on the methods described in Takahashi et al. (2009). For comparison, the data collected from similar locations as WB-7 by Woods Hole Oceanographic Institution (WHOI) (Wang et al., 2017), NOAA Gulf of Mexico and East Coast Carbon cruises 1&2 (Wang et al., 2013; Wanninkhof et al., 2015), and East Coast Ocean Acidification 1 were also included in the analysis.

### Model descriptions

The Coupled Model Intercomparison Project (CMIP) considers various representative concentration pathways (RCPs) that are primarily based on human consumption of fossil fuels (Bopp et al., 2013). Four pathways, namely, RCP2.6, RCP4.5, RCP6, and RCP8.5, are identified according to a possible range of radiative forcing values in the year 2100 (2.6, 4.5, 6.0, and  $8.5 \text{ Wm}^{-2}$ , respectively). The models used for CMIP5 and CMIP6 coarsely resolve the ocean (approximately  $1^\circ$ ) and consequently neglect important coastal processes that can modify global rates of acidification locally in regions like the GOM. However, global models can be used to drive regional higher resolution models designed to resolve coastal processes important for constraining regional rates of acidification and provide important information on how boundary conditions are likely to change. The regional projections used for this work are described in **Table 1**.

Lavoie et al. (2020) projected ocean conditions using a coupled physical–biogeochemical regional climate model, developed for the Gulf of St. Lawrence and the Scotian shelf called the Gulf of St. Lawrence Biogeochemical Model (GSBM; Gehlen et al., 2015), that was driven by three global projections from CMIP5 for the RCP 8.5 scenario. The three ensemble members include the second generation Canadian Earth System Model (CanESM2), the low-resolution version of the Max-Planck-Institut Earth System Model (MPI-ESM-LR), and the latest Hadley Center

**Table 1.** Regional downscaled models used for projecting ocean acidification conditions to 2050. DOI: <https://doi.org/10.1525/elementa.2020.00062.t1>

Model <sup>a</sup>	Downscaling	Representative Concentration			Historical	Future Simulation
		Pathway	Resolution	Ensemble Members <sup>a</sup>	Simulation Period	Simulation Period
GSBM	Dynamical	8.5	6 km (1/12 degree)	CanESM2, HadGEM2-ES, and MPI-ESM-LR	1991–2010	2041–2060
ROMS	Empirical	8.5	7 km	GFDL, IPSL and HadGEM2-ES	1976–2005	2070–2099 and scaled back to 2050

GSBM = Gulf of St. Lawrence Biogeochemical Model; ROMS = Regional Ocean Modeling System; CanESM2 = Canadian Earth System Model; MPI-ESM-LR = Max-Planck-Institut Earth System Model; HadGEM2-ES = Hadley Center Earth System; GFDL = Geophysical Fluid Dynamics Lab; IPSL = Institut Pierre Simon Laplace.

<sup>a</sup>Model abbreviations as provided in the text.



Earth System climate model (HadGEM2-ES) and simulate the period 1970–2100. Future boundary conditions were built by adding the simulated trends from the ESMs to the observed climatology for the physical variables (see Long et al., 2016b, for temperature and salinity), as well as for nitrate, DIC, TA, and dissolved oxygen. The trends from the ESMs that were used to build future boundary conditions for the regional model are generally consistent (Lavoie et al., 2019). The regional model includes the GOM, but the results for that region had not been analyzed until now. Because this model includes biogeochemistry, the projections are referred to as the dynamically downscaled biogeochemical projections.

Other dynamically downscaled projections exist for the GOM as described in Brickman et al. (2021), but most do not include biogeochemistry. A set of simulations were performed using the Regional Ocean Modeling System (ROMS; Shchepetkin and McWilliams, 2005), referred to as ROMS throughout this work, each forced by a global climate model. The model domain covers the entire Northwest Atlantic, including GOM shelf, slope, and the Gulf Stream. The grid is configured with horizontal spacing of approximately 7 km and 40 vertical terrain-following levels (Kang and Curchitser, 2013). A control (CTRL) ROMS simulation was performed using data-assimilated fields at the surface and along the side boundaries in the ocean over the period 1976–2005. The ROMS climate change simulations were performed using the delta method. The deltas were computed by subtracting the long-term monthly mean values during the period 1976–2005 from those during 2070–2099 in each of the three general circulation models: NOAA Geophysical Fluid Dynamics Lab (GFDL), Institut Pierre Simon Laplace (IPSL), and HadGEM. Then, the deltas were added to the CTRL providing three independent future simulations using RCP 8.5 (Alexander et al., 2020). Because the ROMS simulations used 2070–2099 for the future period, the results needed to be adjusted to estimate the changes in 2050. We tested several methods to accomplish this goal using the time-varying CMIP5 simulations, which include values in 2050, to evaluate the accuracy of the adjusted values. A method that worked well uses the global average change in radiative forcing from the RCP8.5 scenario. The change in forcing from 1976–2005 to 2050 is  $3.1 \text{ Wm}^{-2}$  and to 2085 is  $5.68 \text{ Wm}^{-2}$ , so the grid point values of temperature and salinity were scaled by 0.546 ( $3.1/5.68$ ) to estimate the changes that occur by 2050. These results are presented in more detail in Brickman et al. (2021).

To include biogeochemical fields in the projected conditions without dynamic biogeochemistry, an empirical model for the carbonate system to the future conditions was applied and  $\text{CO}_2$  was added to the DIC pool using the atmospheric concentration in 2050 in the RCP scenario, assuming the anthropogenic signal is well mixed throughout the water column. This approach has the benefit that relative contributions of physical changes, like warming, are easily decipherable. An empirical model for each carbonate system parameter was developed using a least-squares multiple linear regression (MLR) of the carbonate

system parameter on hydrographic variable observations collected on the northeast U.S. shelf between 2007 and 2015 (McGarry et al., 2021). Although empirical models including other variables were generated, the models used here rely solely on temperature and salinity but skillfully reproduce observed DIC and TA (McGarry et al., 2021; their Equations I and IV).  $\Omega_a$  was computed from the empirically derived DIC and TA using CO2SYS (Lewis and Wallace, 1998). Additional model evaluation was performed as part of this work, as described below.

Anthropogenic  $\text{CO}_2$  concentrations were added to the DIC computed from the MLR by first calculating the seawater  $\text{pCO}_2$  in equilibrium with the atmospheric concentration in 2050 from RCP 8.5 (550 ppm) using the solubility equations from Weiss et al. (1970) for the projected temperature and salinity. The DIC in equilibrium with future atmospheric concentrations was then computed using the equilibrium  $\text{pCO}_2$  and MLR-computed TA as inputs in CO2SYS (Lewis and Wallace, 1998). The same method was used to calculate DIC for the control conditions and the difference was added to the projected DIC from the MLR. Note that this method will only be representative of the conditions experienced by the training data for the MLR. Because the dynamics of oxygen and carbon are linked, the inclusion of oxygen in the MLR improves the representation of the carbonate system. However, this variable was not available for regional models used here, so the MLR was based on temperature and salinity only. The results of these efforts are reported below and referred to as dynamically downscaled physical projections with empirical biogeochemistry.

#### Model evaluation and metrics

The moored observations described in Salisbury and Jonsen (2018) from Buoy D were used to compare to the base and future projections of the downscaled model. Statistical analyses were used to quantify the comparisons.

*Duration* is defined as the number of months each year that  $\Omega_a$  falls below the critical threshold  $\Omega_{a\beta}$  (1.5). *Intensity* represents the integrated annual acidification stress defined as  $I = \int_{t=1}^{t=12} (\Omega_{a\beta} - \Omega_{a,t}) dt$ , where  $I$  is the intensity,  $\Omega_{a\beta}$  is the threshold (1.5), and  $\Omega_{a,t}$  is the monthly modeled value when  $\Omega_{a,t} < \Omega_{a\beta}$  (i.e., values  $> \Omega_{a\beta}$  are disregarded). This acidification intensity score is similar to other threshold-based stress indices (e.g., degree heating week for gauging coral thermal stress) that adopt the assumption that low-level stress experienced over extended periods can develop into a higher level accumulated stress response similar to that experienced in a short-term chronic or acute stress response. The benefit of the intensity score is that it combines both the magnitude by which the threshold is exceeded as well as the duration.

To determine the role of warming and circulation changes in the future projections of OA, a “slug” of anthropogenic  $\text{CO}_2$  was added to the modern/base case DIC and compared to the projected fields for the ROMS empirical projections. Thus, it yields a modeled field assuming only an increase in DIC in response to OA independent of other changes.

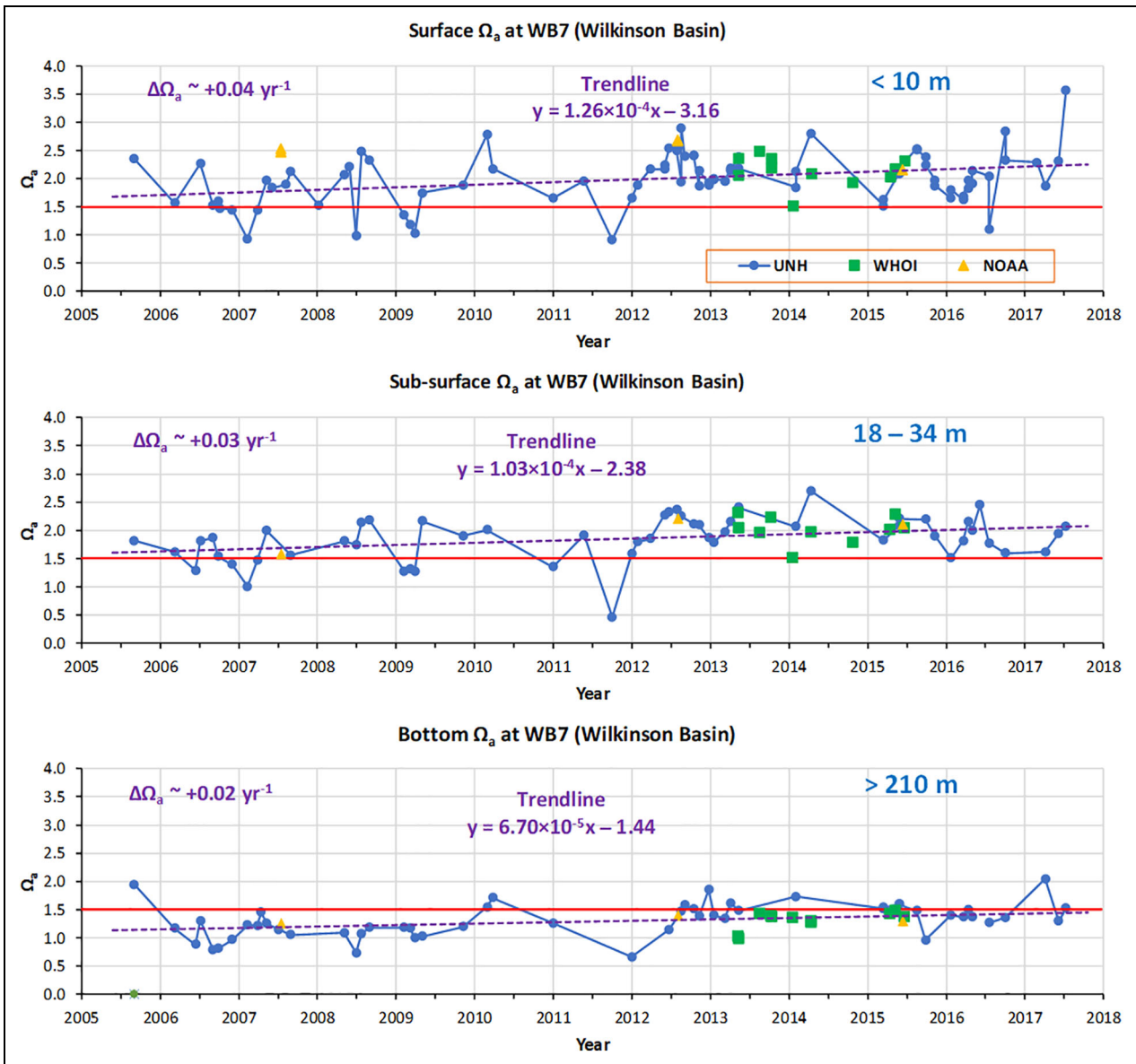


**Figure 3.** Trends of  $\Omega_a$  in offshore surface, subsurface, and bottom waters. Long-term trends of  $\Omega_a$  between 2005 and 2017 for the surface, subsurface, and bottom layers of the water column at a deep station in Wilkinson Basin (WB7; 42.859°N, -69.860°W), Gulf of Maine. Values for  $\Omega_a$  were calculated from dissolved inorganic carbon and total alkalinity data collected from University of New Hampshire (UNH) seasonal transect surveys. Red lines indicate the threshold value  $\Omega_a = 1.5$ . Dashed lines are deseasonalized linear trend lines based on the method of Takahashi et al. (2009). For comparison, WHOI seasonal data (Wang et al., 2017) and NOAA GOMECC 1 (Wang et al., 2013), GOMECC 2 (Wanninkhoff et al., 2015), and ECOA 1 data collected from a nearby location are also shown. Only the UNH data set was used for the trend line analyses. These offshore deseasonalized trends are similar to the surface trend found at the nearshore Buoy D ( $0.015 \text{ yr}^{-1}$  for the period 2004–2015; Salisbury and Jonsson, 2018). NOAA GOMECC = NOAA Gulf of Mexico and East Coast Carbon; ECOA = East Coast Ocean Acidification. DOI: <https://doi.org/10.1525/elementa.2020.00062.f3>

**Observed trends in subsurface  $\Omega_a$**

The UNH repeated transect measurements off the NH coast during the period of 2005–2017 showed that subsurface  $\Omega_a$  from depths of 18–34 m exhibited trends which closely followed those of surface water shallower than 10 m at the deepest station in the WB of the GOM (Figure 3). Bottom water  $\Omega_a$  deeper than 210 m at the same station (WB7, Figure 3) was less correlated with the surface distributions. No clear seasonal pattern of  $\Omega_a$  was observed for either the surface or subsurface offshore

waters, which is consistent with the finding by Wang et al. (2017). Inconsistent sampling frequency of these data might have contributed to the lack of observed seasonality or missed capturing additional shifts or events affecting aragonite saturations, particularly as GOM studies have shown that low  $\Omega_a$  or high  $\text{CO}_2$  events in both surface and bottom waters can dissipate within days or weeks (Waldbusser and Salisbury, 2014). Surface and subsurface waters experience occasional low  $\Omega_a$  conditions at this offshore location below the threshold value ( $\Omega_a = 1.5$ ; red

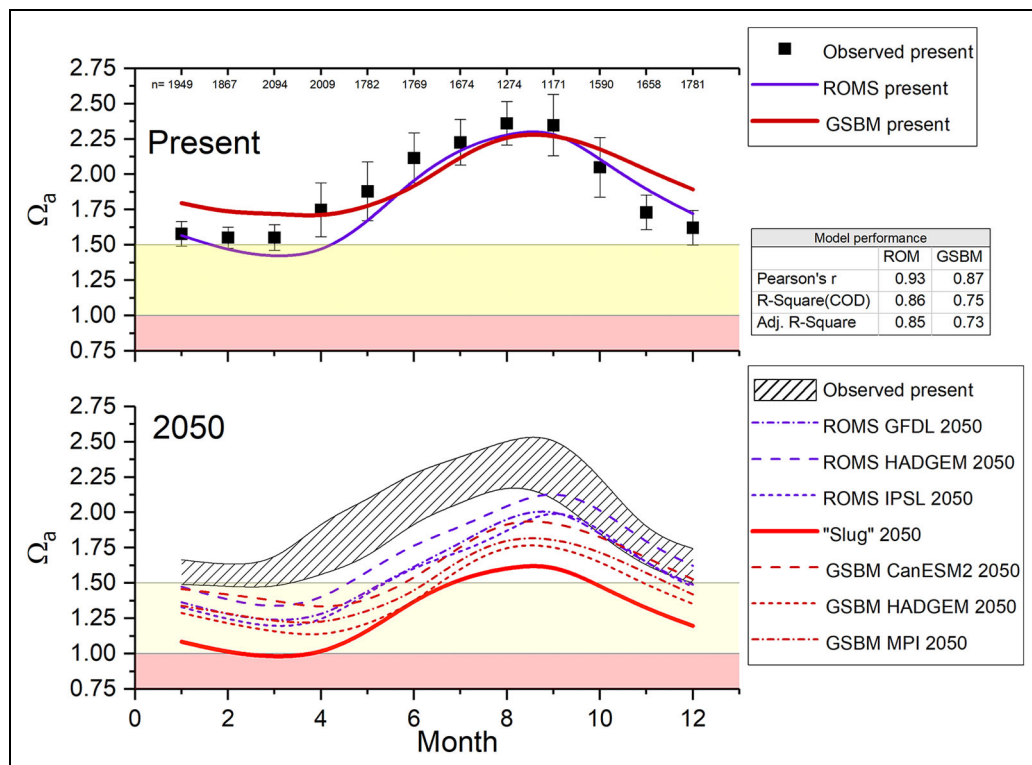


**Figure 4.** Model evaluation and projected conditions of aragonite saturation state ( $\Omega_a$ ) at Gulf of Maine Buoy D. The monthly mean  $\Omega_a$  values for the Pacific Marine Environmental Laboratory/University of New Hampshire Coastal CO<sub>2</sub> Buoy D entire time series (2006–2018) are shown in black squares over a climatological year. The full hourly time series can be seen in Figure 1. The standard deviation of the observations is provided in the upper panel as error bars and as a hatched region in the lower panel with the corresponding  $n$  values for each monthly average on the upper  $x$  axis for the “present” (upper) panel. The yellow-shaded region indicates the region below the threshold of  $\Omega_a = 1.5$ . The red-shaded region indicates the region below the thermodynamically relevant saturation horizon threshold of  $\Omega_a = 1$ . Each of the continuous lines represents a model simulation. The control/present simulations are depicted in the upper panel, while the projected conditions for 2050 are depicted in the lower panel. Statistics regarding model performance in the control/present simulations are provided as an inset table on the upper panel and indicate that the models perform well at this location historically as well as in Figure S2. The future conditions for this location predict that spring and summer will experience much lower values of  $\Omega_a$ , with spring and winter months falling into the yellow region and both time periods outside the range of variability for the past 15 years. The “slug” represents the addition of dissolved inorganic carbon for RCP 8.5 to the present/control conditions for the Regional Ocean Modeling System (ROMS) simulation. The difference between the slug and the ROMS future ensemble conditions represents the continued role of warming and circulation on mitigating future ocean acidification conditions. RCP = representative concentration pathway. DOI: <https://doi.org/10.1525/elementa.2020.00062.f4>

line in **Figure 3**). The observed  $\Omega_a$  values near bottom were persistently below this threshold with only a few exceptions during the 12-year period. A few shorter data sets collected by WHOI and NOAA Ocean Acidification Program generally agree with these patterns (**Figure 3**; Wang et al., 2017). A long-term trend analysis was conducted by subtracting the respective monthly climatological mean  $\Omega_a$  from individual  $\Omega_a$  values in **Figure 3** based on the method of Takahashi et al. (2009). The result shows a positive trend in  $\Delta\Omega_a$  for all three layers of the water column in WB, with an annual increasing rate of 0.02–0.04 per year (**Figure 3**). The rate of  $\Omega_a$  increase at the surface was about twice that of the near-bottom water mass. These trends coincide with (nonsignificant) positive trends in salinity and temperature at the same site (the same colocated data as in **Figure 3**; Figure S2), as well as the  $\Omega_a$  rate estimated for the GOM for the period 2004–

2015 ( $0.0152 \pm 0.003$ ; Salisbury and Jonsson, 2018). These observations confirm that the recent warming and observed salinity increase over the last decade, likely due to the increase of slope water intrusion (Salisbury and Jonsson, 2018), may play an important role in controlling carbonate chemistry in the GOM.

#### Model comparison with observed historical $\Omega_a$

The moored surface observations shown in **Figure 1** from the PMEL/UNH Coastal CO<sub>2</sub> Buoy D, as described in Salisbury and Jonsson (2018), were compared to the down-scaled modeled base and future projections of  $\Omega_a$  (**Figure 4**). The monthly mean values for the entire time series (2006–2018) are shown in black squares and the standard deviation of the observations each month is provided, with additional evaluation provided in Figure S1. The observations indicate that  $\Omega_a$  experiences strong

**Table 2.** GSBM-projected mean  $\Omega_a$  over the Gulf of Maine for 2050 from each ensemble member for surface and bottom waters. DOI: <https://doi.org/10.1525/elementa.2020.00062.t2>

Ensemble Member	Surface		Bottom	
	$\Omega_a$	$\Delta\Omega_a^a$	$\Omega_a$	$\Delta\Omega_a^a$
MPI-ESM-LR	1.69	0.40	1.52	0.36
HadGEM2-ES	1.58	0.42	1.42	0.37
CanESM2	1.76	0.40	1.50	0.37

GSBM = Gulf of St. Lawrence Biogeochemical Model; CanESM2 = Canadian Earth System Model; MPI-ESM-LR = Max-Planck-Institut Earth System Model; HadGEM2-ES = Hadley Center Earth System.

<sup>a</sup>Difference from the control mean: 2.0 for surface, 1.79 for bottom.

seasonality at this location, with higher values at the surface during summer and lower values during winter, which can also be seen in **Figure 1**. Presently, surface conditions away from the shore rarely experience suboptimal conditions for marine organisms and rarely decline below the saturation horizon (**Figures 1 and 4**).

Both of the downscaled models used for the projected conditions in this work perform well when compared to the historical observations of  $\Omega_a$  (GSBM:  $R^2 = 0.75$ ; ROMS:  $R^2 = 0.86$ ; **Figure 4**). GSBM underestimates the seasonality of the observations, with slightly higher saturation states in the winter than observed, although that is the observed trend. In the spring, ROMS with empirical biogeochemistry likely underestimates the role of the spring bloom in raising the  $\Omega_a$  by scavenging DIC from the surface mixed layer, and so the model underestimates the saturation state at that time. As a result, winter and spring projections are more uncertain as they are not as well simulated in the model suite. Despite these minor inconsistencies, the ability of the models to capture the historical climatological conditions suggests that they are robust enough to reasonably project future conditions.

The empirical biogeochemical model can also be applied to the GSBM simulation to understand the relative importance of the physical simulation in GSBM to the biogeochemical feedbacks. The GSBM model control simulation produces a surface average  $\Omega_a$  for the GOM of 1.68 and 1.48 at the bottom. When the empirical biogeochemistry is applied to the GSBM temperature and salinity fields, the mean surface  $\Omega_a$  for the control simulation is 1.84, and the bottom is 1.63. Both of the results from the empirical biogeochemical model produce higher saturation states than the dynamic biogeochemical model.

### OA projections for the GOM for 2050

#### Global projections

The CMIP5 ensemble average under RCP 8.5 projects a decline in  $\Omega_a$  of 0.44 at the surface (not shown) for the entire GOM region when the control values (for the period 1976–2005) are subtracted from the average for the

future (2005–2055). When the MLR is applied to the temperature and salinity from the CMIP5 future projection, the projected decline is reduced (0.17). In the subsurface, the global models only simulate bottom conditions at the shallowest around 300-m depth and no longer serve the DIC and TA values for the region, so the MLR method is used. Using that depth as representative of the bottom conditions projected for the GOM, the CMIP5 ensemble average for the GOM projects a decline in  $\Omega_a$  of 0.15.

#### Dynamically downscaled biogeochemical projections

Surface and bottom  $\Omega_a$  decline in the future in the GSBM projections for 2050 under RCP 8.5. The decline at the surface is projected to be 0.40 for the MPI-ESM-LR and CanESM2 forced projections and 0.42 for the HadGEM2-ES ensemble member (**Table 2**). The ensemble members largely agree on the magnitude and direction of the trend. Bottom conditions are largely consistent with the surface, with a slightly weaker decline (0.36–0.37; **Table 2**). Although the surface is comparable to the global model projected change, the subsurface change is larger than the global models, in part due to the lack of resolution over these depth ranges in the global models. In addition to the future projected changes, the absolute values for  $\Omega_a$  in the global model are higher than in the downscaled models predicted in both the control (C) and future (F) simulated conditions, that is, C:2.73 and F:2.29 versus C:2.00 and F:1.68.

The decline in  $\Omega_a$  is driven in the regional model mainly by the increase in DIC in the region, which occurs at all depths and in all three simulations (**Figure 5**). We note that increasing DIC is mainly attributable to increasing atmospheric  $\text{CO}_2$  but may also be imported into the region or result from increasing rates of respiration with warming conditions. The DIC increase is greatest at depth. The decrease in pH in the 150–300 m layer is greater in the GOM than in the Scotian Shelf or GSL (Lavoie et al., 2020) because the DIC increase is greater in the GOM. The model suggests that this difference is caused by an increase in primary production, mainly by diatoms, and greater mesozooplankton mortality in summer due to higher water temperatures, with both leading to an increase in local respiration of organic matter at depth in the region. Stratification is also stronger in the projection which reduces the ventilation of subsurface waters.

Alkalinity generally decreases at the surface and increases in all the regional simulations at depth (150–300 m; **Figure 6**). The surface trends differ widely among the three ensemble members in magnitude with HadGEM2-ES producing the steepest decline in TA, and due to this disagreement, the trends are highly uncertain at the surface and midwater column (**Figure 6A and B**). These changes in alkalinity primarily correspond to the changes in salinity in the region with fresher surface waters and saltier deep waters.

Because the results were simulated continuously between 1970 and 2100, the simulations project the timing when key thresholds are exceeded in the region. Like pH,  $\Omega$  continues to decline under RCP 8.5. For key thresholds, like  $\Omega_a$  and saturation state for calcite, the

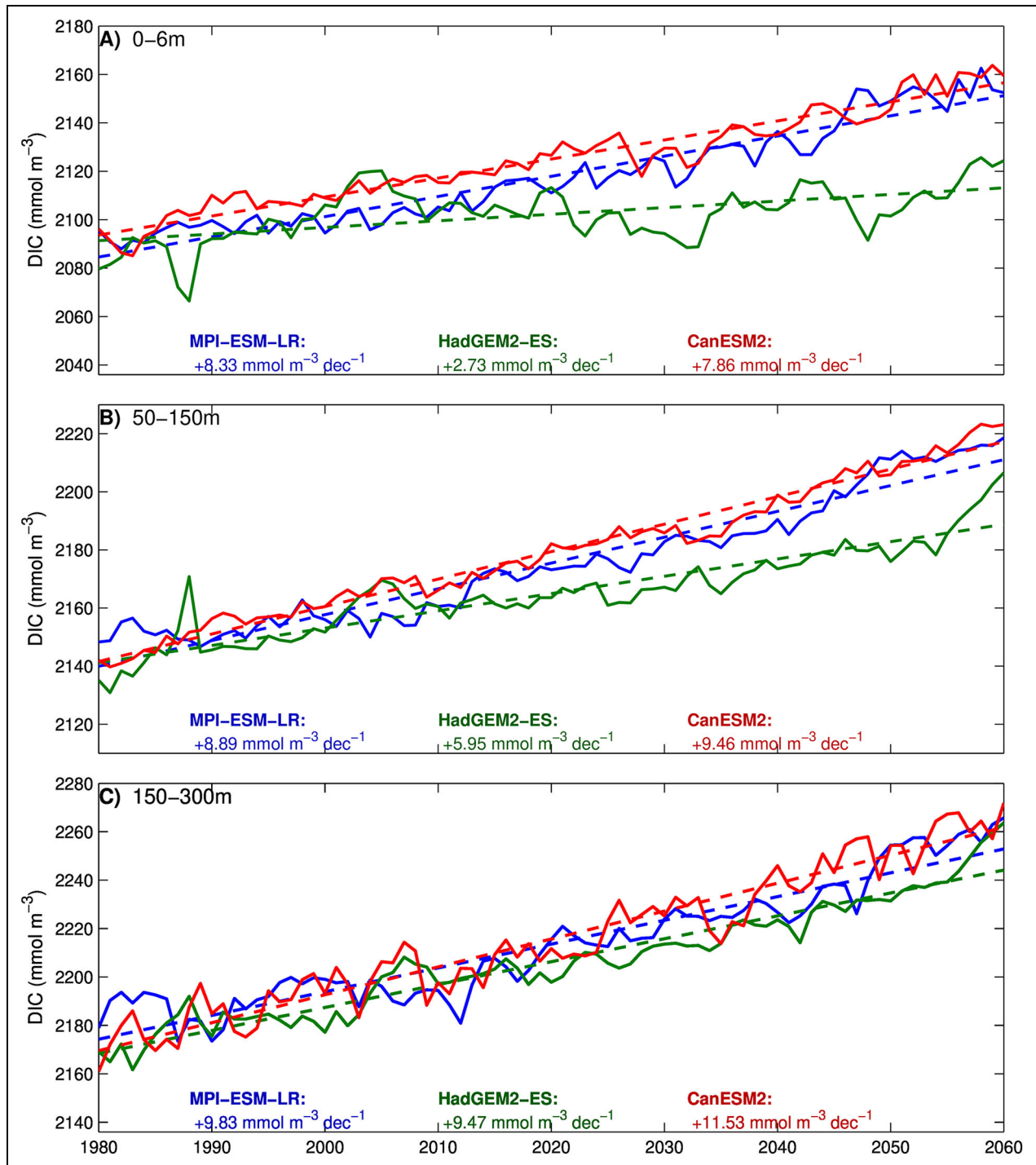
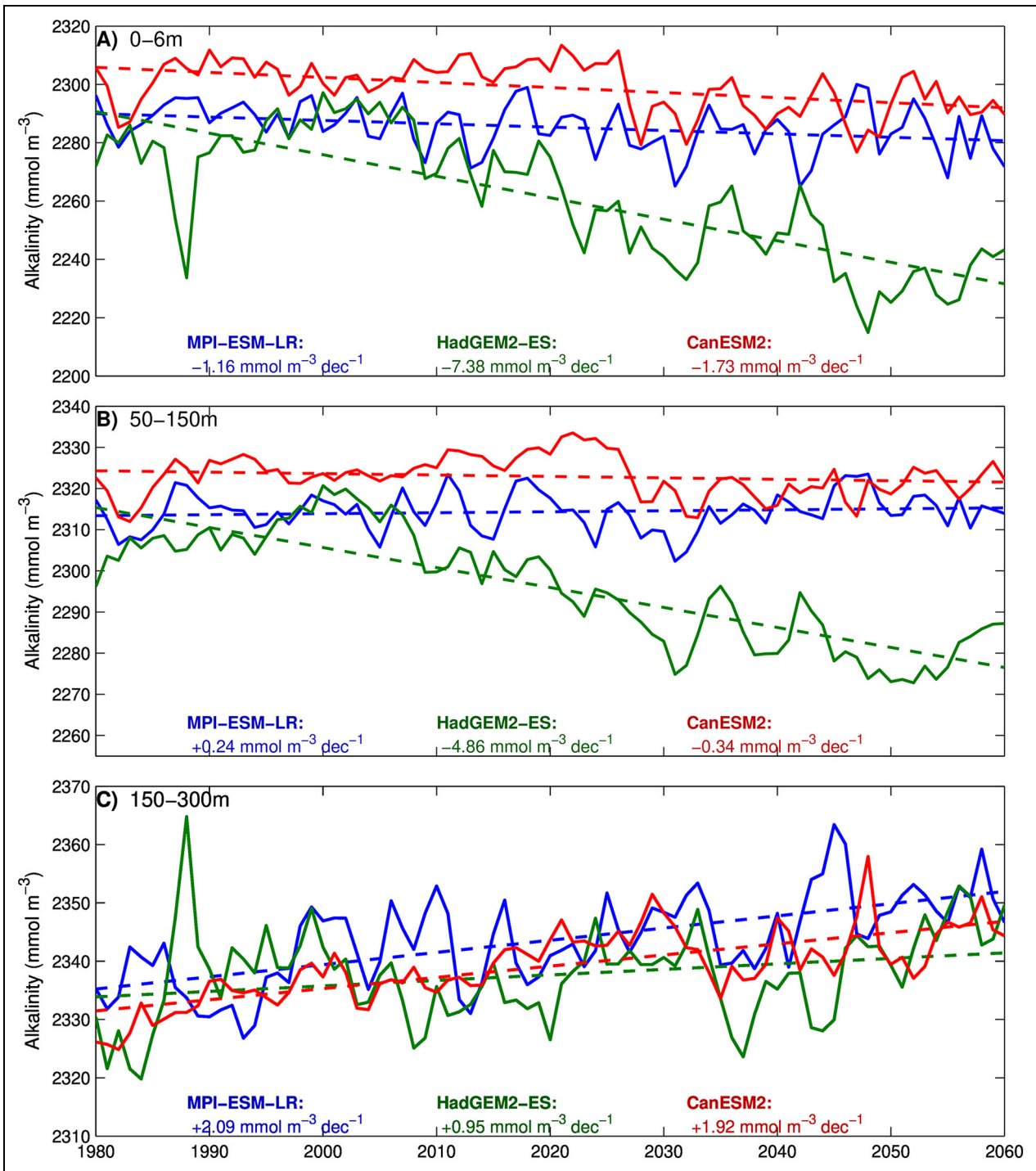


**Figure 5.** Time series of dissolved inorganic carbon (DIC) concentration at three depth layers from the Gulf of St. Lawrence Biogeochemical Model (GSBM). Mean DIC concentrations from the GSBM model for the Gulf of Maine region from a continuous simulation from 1970 to 2070 for the depth layers of (A) 0–6 m, (B) 50–150 m, and (C) 150–300 m. Each ensemble member is color coded with the corresponding rate of increase per decade provided on each graph. The ensemble members largely agree subsurface and then diverge closer to the surface with Hadley Center Earth System (HadGEM2-ES) reporting the slowest rate of increase at the surface. HadGEM2-ES also reports the greatest warming over the time interval. DOI: <https://doi.org/10.1525/elementa.2020.00062.f5>

thermodynamic threshold of 1 (annual mean) is reached in the benthic environment in all three ensemble members by the year 2060 in the southern GOM for aragonite. By 2081, calcite remains above saturation for the entire domain. Suboptimal  $\Omega_a$  conditions of less than 1.5 are projected for the surface by 2040–2060 with some

uncertainty between the simulations and already present in the benthic environment by 2020 for aragonite and by 2060 for calcite in the southern portion of the GOM (Figure 7). Georges Bank is a region that remains above the threshold for the longest period of time, and one (CanESM2) ensemble member entirely avoids the



Downloaded from <http://online.ucpress.edu/elementa/article-pdf/9/1/00062/462357/elementa.2020.00062.pdf> by guest on 07 June 2021

**Figure 6.** Time series of total alkalinity (TA) concentration at three depth layers from the Gulf of St. Lawrence Biogeochemical Model (GSBM). Mean TA concentrations from the GSBM model for the Gulf of Maine region from a continuous simulation from 1970 to 2070 for the depth layers of (A) 0–6 m, (B) 50–150 m, and (C) 150–300 m. Each ensemble member is color coded with the corresponding rate of change per decade over the time interval provided on each graph. The ensemble members largely agree subsurface and then diverge closer to the surface with Hadley Center Earth System (HadGEM2-ES) reporting the fastest rate of decline at the surface. HadGEM2-ES also reports the greatest warming and freshening over the time interval. The model predicts that surface and subsurface waters will experience different directional trends in TA over this time period with the surface and mid-depth experiencing a decline in TA and the subsurface experiencing an increase. This pattern is suggestive of different water mass influences in the region with freshwater driving the surface trends and water masses more similar to the Gulf Stream driving the subsurface increase. DOI: <https://doi.org/10.1525/elementa.2020.00062.f6>

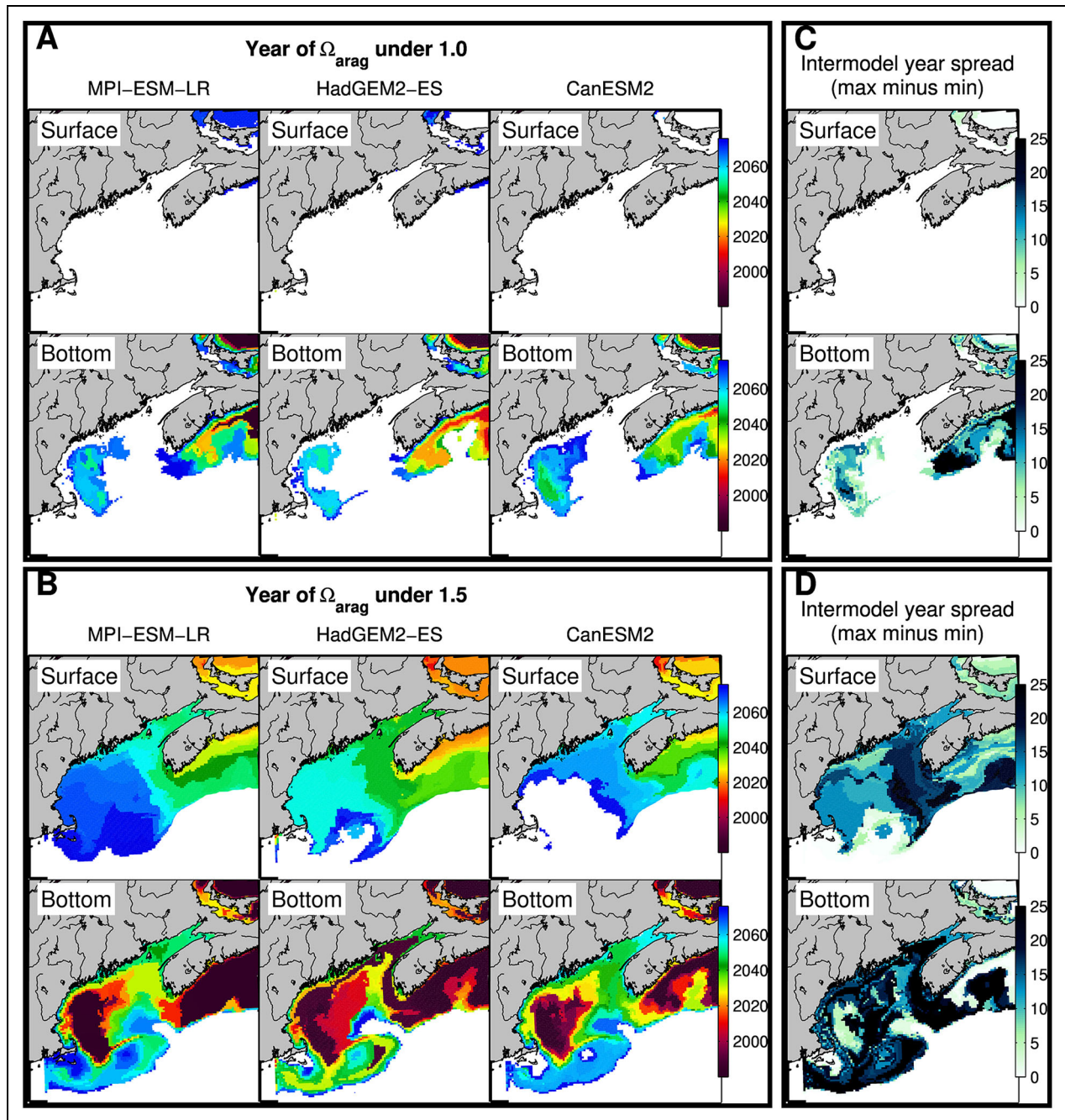


**Figure 7.** Time of emergence for conditions of  $\Omega_a < 1.5$  from the Gulf of St. Lawrence Biogeochemical Model (GSBM). Aragonite saturation state ( $\Omega_a$ ) conditions from the GSBM model for the Gulf of Maine from a continuous simulation from 1970 to 2070. Color-coded contours in the left panels (A and B) indicate the year when saturation state falls below the threshold of  $\Omega_a = 1$  (A) and  $\Omega_a = 1.5$  (B) in the annual mean from each ensemble member for surface (upper row) and bottom (lower row) water conditions. The intermodel spread (max – min) is also mapped in the right panels (C and D) as a measure of uncertainty. DOI: <https://doi.org/10.1525/elementa.2020.00062.f7>

threshold at the surface. As such, Georges Bank is one of the regions of largest disagreement between the ensemble members. The Scotian Shelf is one of the regions that experiences the earliest threshold crossing in the domain at both the surface and the bottom.

#### *Dynamically downscaled physical projections with empirical biogeochemistry*

Consistent with the dynamical biogeochemical model results from GSBM, the surface and bottom  $\Omega_a$  conditions

are also projected to decline with the empirical biogeochemistry results (**Table 3**). The surface  $\Omega_a$  decline is projected to be 0.12 and 0.14, respectively, from the GFDL and IPSL forced ensemble members and 0.03 for the HadGEM simulation. The bottom  $\Omega_a$  decline is projected to be 0.11 and 0.15, respectively, for the GFDL and IPSL forced ensemble members and 0.02 for the HadGEM simulation. These changes are smaller than projected by the dynamical biogeochemistry GSBM model and not as similar with respect to depth. However, the empirical biogeochemical

**Table 3.** ROMS-projected mean  $\Omega_a$  over the Gulf of Maine for 2050 from each ensemble member for surface and bottom waters. DOI: <https://doi.org/10.1525/elementa.2020.00062.t3>

Ensemble Member	Surface		Bottom	
	$\Omega_a$	$\Delta\Omega_a^a$	$\Omega_a$	$\Delta\Omega_a^a$
GFDL	1.61	0.14	1.44	0.11
HadGEM	1.72	0.03	1.53	0.02
IPSL	1.60	0.12	1.40	0.15

ROMS = Regional Ocean Modeling System; GFDL = Geophysical Fluid Dynamics Lab; HadGEM = Hadley Center; IPSL = Institut Pierre Simon Laplace.

<sup>a</sup>Difference from the control mean: 1.75 for surface, 1.55 for bottom.

CTRL conditions are lower than the GSBM model. When the empirical model is applied to the GSBM temperature and salinity values for the projection, the projected decline in surface  $\Omega_a$  for the mean change across all three ensemble members in the GOM is 0.37 and, in the bottom, 0.20, suggesting that even in those simulations, the empirical model does not support uniform change vertically in the future. Although the surface is comparable to the global model MLR-based projected change (0.17) and lower than the decline projected by the DIC and TA-based projections (0.44), the subsurface declines less severely for two ensemble members (0.02 and 0.11; **Table 3**) or consistently for one ensemble member (0.15; **Table 3**) when compared to the global model projected change (0.15; **Table 3**). In addition, the absolute values for  $\Omega_a$  in the global model (C:2.04, F:1.87) are higher than in the down-scaled models (C:1.75, F:1.64) predicted in both the control and future simulated conditions.

Under RCP 8.5 in 2050, the ROMS model ensemble projects that persistently suboptimal conditions for marine organisms (i.e.,  $\Omega_a < 1.5$ ) will exist at the surface for the first 5 months of the year (January–May; **Figure 4**). Maximum supersaturation will shift from late summer (August) to early fall (September). One of the three ensemble members (HadGEM) does not project as severe a seasonal evolution, with fewer months experiencing suboptimal conditions for marine organisms (i.e.,  $\Omega_a < 1.5$ ), because it is the projection with the warmest temperatures which continue to counteract the effects of OA. This shift in the presence of undersaturated waters in the spring and the timing of maximum saturation state later in the year may have biological impacts, as these seasonal transitions often correspond to reproductive and early life stage transitions in many marine organisms, which are typically more vulnerable to OA.

Projected conditions for 2050 are very different from control conditions for RCP 8.5 in terms of DIC for all three ensemble members (**Figure 8**). However, in all cases, DIC anomalies are highest offshore and lowest near the coast. Although the magnitude varies across ensemble members, the fall produces the sharpest gradients in the anomaly

between the coast and offshore and experiences the most variability between ensemble members. In all three ensemble members, using the empirical model alone without the adjustment for the higher atmospheric CO<sub>2</sub> concentrations or the “slug,” DIC concentrations are less than modern conditions (not shown), suggesting that physical changes to the GOM along with biological feedbacks are acting to mollify the increases from the atmospheric change.

All three ROMS simulations experienced lower TA at the surface (**Figure 9**), consistent with the projected salinity and dynamically downscaled biogeochemical projections described above. Subsurface TA increases in the future, consistent with the GSBM results. Seasonally, the late fall conditions (October–December) experienced the greatest magnitude of change, although the three simulations vary widely in the magnitude of the changes.

### Implications of OA for the GOM

Biologically relevant impacts from OA, particularly for shell-forming organisms, can be interpreted from the duration of exposure to conditions below the identified  $\Omega_a$  threshold of 1.5 (i.e., number of months when  $\Omega_a$  is  $< 1.5$ ) as well as the intensity of exposure (magnitude below  $\Omega_a$  1.5). Currently, the maximum duration of exposure in the modern baseline model at the surface does not exceed 4 months (“CTRL” in **Figure 10**) and is concentrated nearshore, with some of the southern GOM region further offshore experiencing approximately a month of exposure. In the future projections for 2050 under RCP 8.5, the maximum duration of nonoptimal exposure at the surface continues to be in the nearshore but is longer (6–8 months) and expands spatially to include the majority of GOM surface waters, with approximately 4 months of exposure. The ensemble members project a range of conditions, with the IPSL projection providing the most severe duration and HadGEM projecting the smallest duration encompassing the smallest subsurface area.

At the bottom, baseline control conditions are more severe than at the surface, and the majority of the GOM experiences below-threshold conditions for nearly half the year with the WB experiencing year-round exposure. In the 2050 projections, the duration of below-threshold conditions increases to year-round over the majority of the region, with the exception of Georges Bank where it increases from 4 months year<sup>-1</sup> in the control to 8 months year<sup>-1</sup> (**Figure 10**).

Intensity of exposure at the surface is tightly coupled to the nearshore coastline in the modern baseline (“CTRL” in **Figure 11**). In the future, the intensity of exposure becomes more severe along the coastline and spreads over the GOM with a wide range projected among the ensemble members. The disagreement between the projections stems from the degree of warming simulated in each of the projections, with HadGEM projecting the most intense warming and thus the least severe intensity of  $\Omega_a < 1.5$ . Georges Bank remains one of the most favorable environments in the GOM region, remaining largely above the threshold. The difference between the “slug” and the future ensemble conditions illustrates the partial



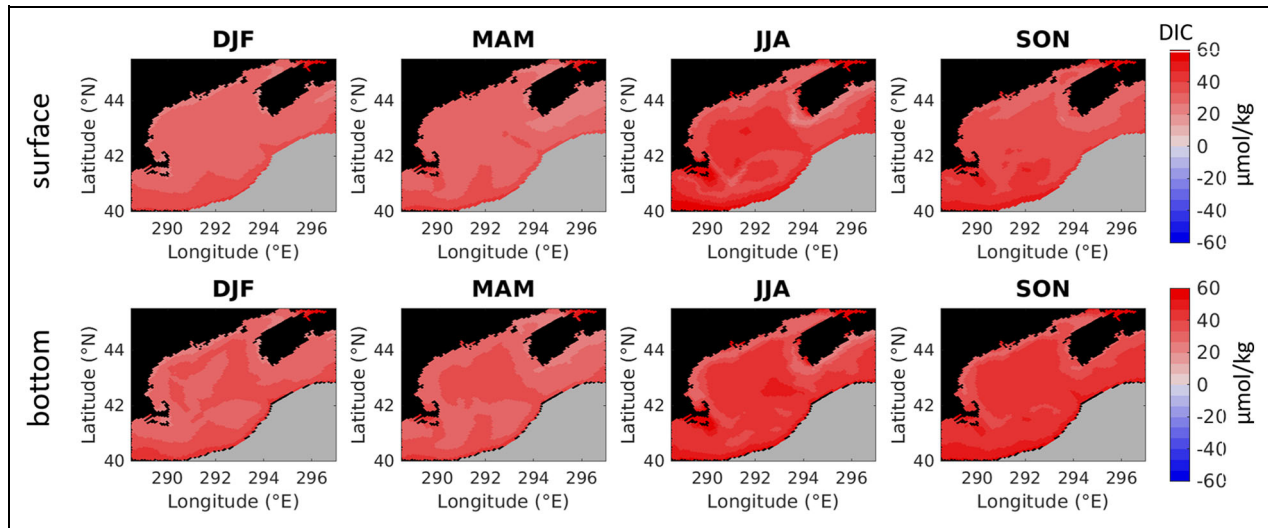


**Figure 8.** Dissolved inorganic carbon (DIC) seasonal anomalies from the Regional Ocean Modeling System model with empirical biogeochemistry. Seasonal maps of DIC in surface (upper panels) and bottom (lower panels) waters for the future (2050) minus control (CTRL) anomaly in the Gulf of Maine. Seasons are divided as December–February (DJF), March–May (MAM), June–August (JJA), and September–November (SON). Color bar DIC units are  $\mu\text{mol kg}^{-1}$ . CTRL conditions are plotted in Figure S7. DOI: <https://doi.org/10.1525/elementa.2020.00062.f8>

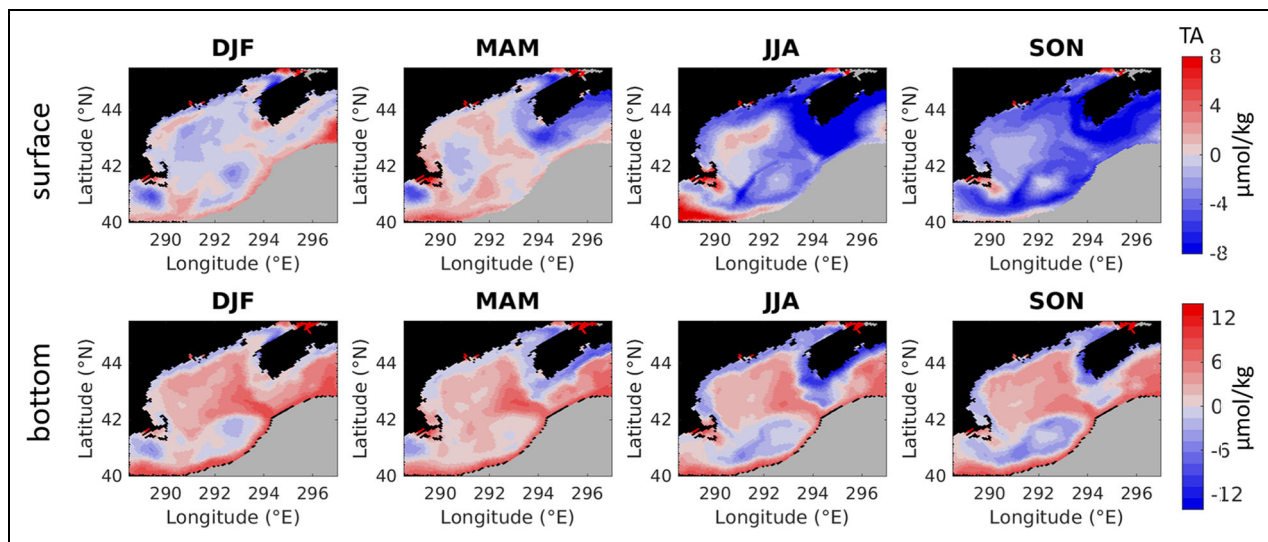


**Figure 9.** Total alkalinity (TA) seasonal anomalies from the Regional Ocean Modeling System model with empirical biogeochemistry. Seasonal maps of TA in surface (upper panels) and bottom (lower panels) waters for the future (2050) minus control (CTRL) anomaly in the Gulf of Maine. Seasons are divided as December–February (DJF), March–May (MAM), June–August (JJA), and September–November (SON). Color bar TA units are  $\mu\text{mol kg}^{-1}$ . CTRL conditions are plotted in Figure S6. DOI: <https://doi.org/10.1525/elementa.2020.00062.f9>

compensation that continued warming and circulation changes impart on future OA conditions, which partly limit acidification intensity at the surface and even more so at depth (Figure 11).

Results indicate that warming continues to partly reduce the impacts of OA in the future as demonstrated by the “slug” compared to the projected change for the region (Figures 4, 10, and 11). Under the RCP 8.5 scenario, both intensity and duration of below-threshold conditions would be more severe in the GOM in 2050 without the additional warming and circulation changes (Figure

S2). The duration doubles without the amelioration of circulation and warming, and the intensity score ( $I$ ) is a full unit more severe. The slug map indicates that the warming and circulation act to mollify the OA duration, particularly in the nearshore surface environment and more so than at the bottom (Figure 10).

## Discussion

Regional high-resolution downscaled projections for the GOM of  $\Omega_a$  conditions inclusive of coastal processes under RCP 8.5 project that the entire region is likely to

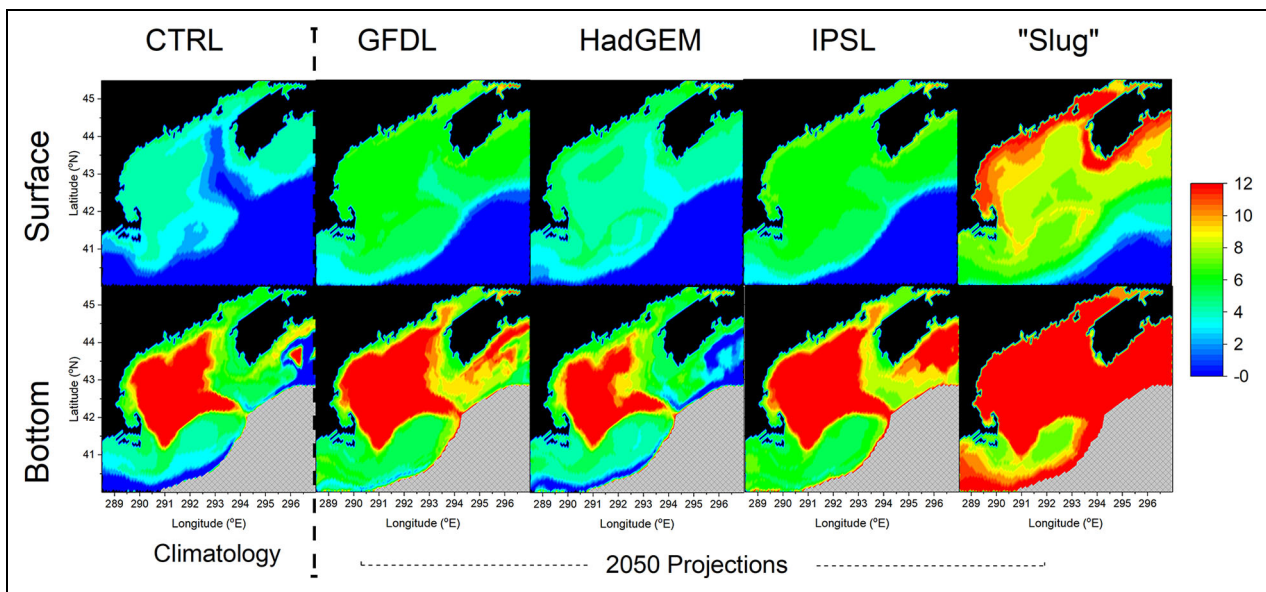


**Figure 10.** Acidification duration score from the Regional Ocean Modeling System simulations with empirical biogeochemistry. Duration of exposure to low saturation state conditions for the baseline control (CTRL; 1991–2010) conditions as well as future projections for 2050 (2041–2060) under RCP 8.5 for each ensemble member for surface (upper panels) and bottom (lower panels) waters. *Duration* is defined as the number of months each year that  $\Omega_a$  falls below the critical threshold of  $\Omega_a = 1.5$  and has units of months per year. The “slug” represents the addition of dissolved inorganic carbon for RCP 8.5 to the control conditions. The difference between the slug and the future ensemble conditions represents the continued role of warming and circulation on mitigating future ocean acidification conditions. The baseline exposure nearshore does not exceed 4 months year<sup>-1</sup> anywhere in the region at the surface. In bottom waters, baseline control conditions are more severe than at the surface, and the majority of the Gulf of Maine experiences below-threshold conditions for nearly half the year with the Wilkinson Basin experiencing year-round exposure. RCP = representative concentration pathway. DOI: <https://doi.org/10.1525/elementa.2020.00062.f10>

experience  $\Omega_a < 1.5$  by 2050. These projections are in contrast to the CMIP5 projections for the region, particularly in the subsurface environment, which predict a decline in future  $\Omega_a$ , but the projected values do not fall below the  $\Omega_a = 1.5$  threshold over much of the region by 2050. Subsurface waters are not well represented by coarse global models, yet house many important shellfish species in the region. In the discussion that follows, we first put the projected results in the context of prior projections for the region. We compare the models used in this work and suggest which processes are vital to best reduce uncertainties in model projections moving forward. We also consider the implications of the results for the vulnerable ecosystems of the GOM, with a particular focus on the nearshore and subsurface environments and economically important species. Finally, we summarize adaptive societal measures that could be employed in the region to potentially avert or mitigate these future changes.

Globally, the oceans simulated using CMIP5 under RCP 8.5 are projected to be higher in  $p\text{CO}_2$  and more acidified (surface pH decrease of  $-0.33 \pm 0.003$ ; Gattuso et al., 2015). Regionally, the direction of the trend predicted here is the same, but there are differences between the global and downscaled results, mostly on the subsurface shelf which is home to many valuable shellfisheries in the region including scallops. Prior projections used to assess

OA impacts to the scallop fishery in the region relied on the global model projections from CMIP5 and did not report  $\Omega_a$  (Rheuban et al., 2018), but the previous iteration of that study by Cooley et al. (2015) reported deep box  $\Omega_a$  values that were greater than those reported here. Our summary of CMIP5 projections for the region suggests that the benthic habitat where adult shellfish reside will endure more severe change in the future than previously estimated.

Global coarse resolution model projections differ from the regional projections discussed here because the intrusion of anthropogenic  $\text{CO}_2$  is not the only mechanism that can reduce  $\Omega_a$  within coastal surface waters. Local processes like freshwater delivery, eutrophication, productivity, and sediment interactions that drive variability on regional and subseasonal scales can also modify spatial variability in  $\Omega_a$  (Feely et al., 2008, 2018; Cai et al., 2011; Qi et al., 2017; Siedlecki et al., 2017; Pilcher et al., 2018). Although the downscaled simulations presented here do not simulate the highly variable and more severe nearshore  $\Omega_a$  conditions depicted by the CML observations in **Figure 1**, the shelf variability is well captured by the models. The downscaled surface trends are comparable to the global model projected change, but the subsurface change is larger than projected by the global models, suggesting that there are processes in the downscaled simulations amplifying this rate of change within

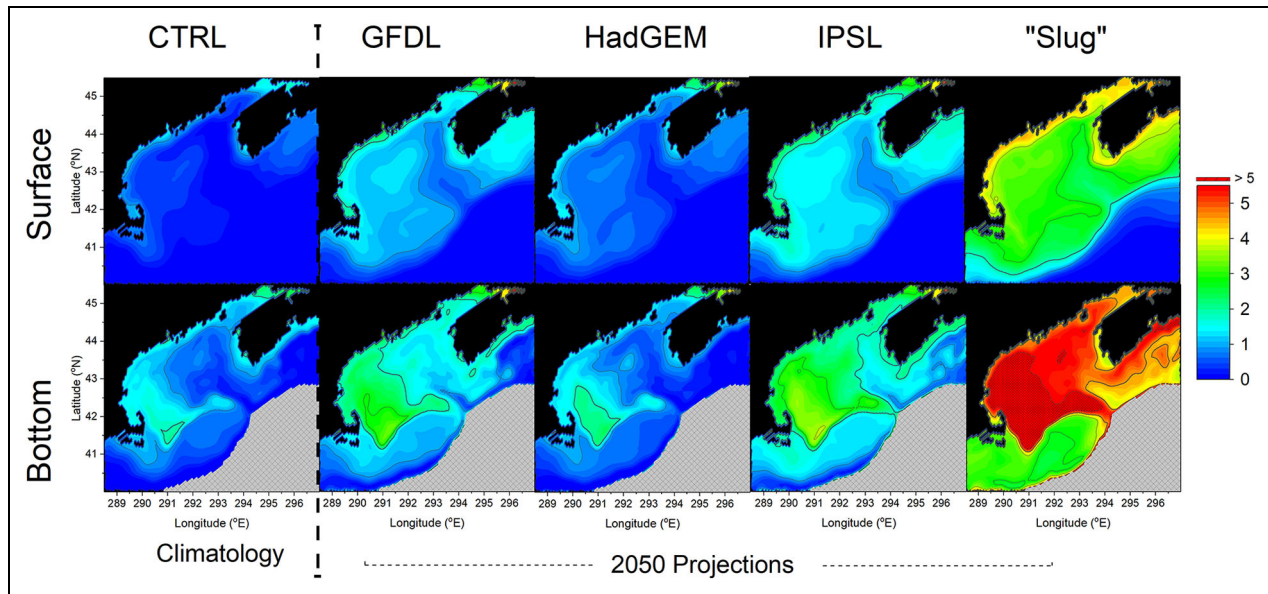


**Figure 11.** Acidification intensity score from the Regional Ocean Modeling System simulations with empirical biogeochemistry. Intensity of exposure to low saturation state conditions for the baseline control (CTRL; 1991–2010) conditions as well as future projections for 2050 (2041–2060) under RCP 8.5 for each ensemble member for the surface (upper panels) and bottom (lower panels) waters. *Intensity* represents the annual integrated acidification stress below the critical threshold of  $\Omega_a = 1.5$ , as described in the methods. At the surface in the CTRL conditions, the nearshore coastline experiences the greatest intensity, albeit relatively weak. The bottom conditions in the CTRL are slightly more intense. Georges Bank remains one of the least intense regions in the Gulf of Maine. The “slug” represents the addition of dissolved inorganic carbon for RCP 8.5 to the control conditions. The difference between the slug and the future ensemble conditions represents the continued role of warming and circulation on mitigating future ocean acidification conditions, which are modifying the intensity at the surface and even more so at depth. RCP = representative concentration pathway. DOI: <https://doi.org/10.1525/elementa.2020.00062.f11>

this critical habitat for scallops, lobsters, and other vulnerable benthic dwellers. Such processes could include those previously reported (e.g., water column metabolism and sediment interactions), but additional research is needed to understand the role of these processes on decadal timescales. Additionally, existing projections, including the ones presented here, should be used as conservative estimates for nearshore environments as they already experience sub-optimal conditions for marine organisms (**Figure 1**) more severely than regions offshore in the GOM.

Differences exist between the regional projections using dynamical biogeochemistry and the empirical biogeochemistry, and those differences can be exploited to prioritize observation needs and process-based understanding of potential biogeochemical feedbacks for future work. The empirical model of biogeochemistry assumes the net biological and sedimentary flux contributions at present will be similar in the future. Differences between the empirical and dynamic biogeochemical model projections suggest that the balance of those processes may change and result in biogeochemical feedbacks in the future. Here, the projections differ in their vertical structure for future change: The surface experiences the same amount of change, but the subsurface is projected to decline more in the dynamical biogeochemistry in conjunction with the surface. This effect likely results from a biogeochemical feedback but could also correspond to

altered residence times due to circulation changes in the region relating to weakening of the Gulf Stream, as is further described in Alexander et al. (2020). The ROMS projections used here and in Alexander et al. (2020) show an enhanced counterclockwise circulation in the region in the future which could alter the residence time of the water masses and thus their effective age. The dynamical model (GSBM) results indicate an increase in primary production, mainly by diatoms, and a greater mesozooplankton mortality in the summer of 2050 due to the higher water temperature, which both lead to an increase in local respiration of organic matter at depth in the region. Increase in local subsurface respiration would cause a further decline in  $\Omega_a$ . This kind of feedback is not represented by the empirical biogeochemistry but could be resolved by monitoring the biomass and rates of net primary and secondary production, along with their interactions with changing hydrographic conditions in the region. Targeted research to constrain these uncertainties would increase confidence in the biogeochemical model response and reduce uncertainties in the projections.

The ensemble spread of the downscaled simulations represents a measure of uncertainty in the system for the projected future conditions. The ensemble spread was small for the GSBM projections as the projected conditions largely agree in both the absolute values for future  $\Omega_a$  and the magnitude of the change from present.

However, the absolute values for the surface and bottom projections did vary based on the degree of warming, mostly per ensemble member (**Table 2**). ROMS ensemble spread is similar for the surface and subsurface, with the HadGEM-forced simulation which has the warmest SST projection producing the smallest change from the control. The HadGEM forced simulation also projects the highest  $\Omega_a$  in the future (**Table 3**). The decline in  $\Omega_a$  from control conditions due to the addition of anthropogenic CO<sub>2</sub> for 2050 under RCP 8.5 is  $-0.22$  to  $-0.29$  across the ROMS ensemble, and the majority of that is compensated by the future warming ( $+0.16$  to  $+0.25$ ). The most compensation is provided by the warmest ensemble member, HadGEM. Salinity changes in the future act to further reduce  $\Omega_a$ , but the magnitude of this change is small on an annually averaged basis ( $-0.01$ ). As a result, reducing the uncertainty surrounding the future warming and rates of warming in the region is essential to reducing the uncertainty on the OA projections.

All the downscaled simulations agree that the region will experience more suboptimal conditions for marine organisms for the majority of the year by 2050 in both the surface and bottom conditions. The degree to which this change occurs is modulated by the degree of projected warming and freshening in the physical simulations. All three simulations of the ROMS model projected large increases in SSTs and changes in bottom water temperature over most of the domain (Alexander et al., 2020; Brickman et al., 2021). The enhanced warming may result from a number of processes discussed in Alexander et al. (2020) including very strong warming of the atmosphere over eastern Canada that is transported over the Atlantic by westerly winds, heating the ocean via changes in the surface fluxes. In addition, strong warming occurs in portions of the North Atlantic, especially to the southeast of Newfoundland, which are subsequently advected into the GOM including through the NEC. In all simulations, the Gulf Stream is projected to be weaker (Alexander et al., 2020). Reducing the uncertainty surrounding rates of warming in the future would also reduce the uncertainty in the OA projected conditions.

Over the past 15 years, waters in the GOM have taken up CO<sub>2</sub> at a rate significantly slower than that observed in the open oceans due to a combination of the extreme warming experienced in the region and an increased presence of well-buffered Gulf Stream water (Salisbury and Jonsson, 2018). The reduced uptake of CO<sub>2</sub> by the region has also altered local acidification rates, which differ from the global rates in the GOM. In Salisbury and Jonsson (2018), the rates, averaged for the entire GOM from 1981 to 2014, showed a decline in  $\Omega_a$  at the surface of  $-0.049$  ( $\pm 0.009$ ) per decade, which is slower than global declines of  $\Omega_a$  and falls outside the range reported over many sites around the world ( $-0.0066$  to  $-0.0115$  per year, 1982–2012; Bates et al., 2014). When the time period is limited to 2004–2015 when observations were in place at Buoy D and warming was greatest in the region, the  $\Omega_a$  increase at the surface was 0.015 per year, which is consistent with the WB observational trends reported here for the subsurface (0.02–0.04 per year; **Figure 3**). These

trends correspond to a time period when the region became increasingly dependent on vulnerable shellfish fisheries (Gledhill et al., 2015; Figure S1). In the projections presented here, the GSBM model simulates a constant rate of  $\Omega_a$  decline of  $-0.008$  per year over the upper 150 m between 1980 and 2060. In a companion paper about the future warming for the region using the same simulations discussed here (Brickman et al., 2021), warming continues to be projected and continues to ameliorate the impacts of OA in the region. However, under RCP 8.5, the impacts of OA still emerge in our projections by 2050 over the entire region with implications expected for the vulnerable ecosystems that reside in the GOM.

Developing knowledge on life stage and population-specific impacts of OA on marine organisms is critical to projecting vulnerabilities and developing adaptation plans for marine biodiversity and for sustaining ecosystems and the socioeconomically dependent coastal communities that rely on these resources. Multiple aspects of the carbonate system have been shown to have impacts on marine biota. Reductions in CO<sub>3</sub><sup>2-</sup> availability and  $\Omega_a$  below critical thresholds have been shown to represent a stressor to a variety of shelled marine invertebrates (e.g., Clements et al., 2017, 2018; Rheuban et al., 2018; Young and Gobler, 2018; Pousse et al., 2020) including crabs, lobsters, oysters, scallops, and mussels in the GOM (Tables S1 and S2). The pH can impact physiological processes that rely on the transfer of [H<sup>+</sup>], including olfactory senses in fish (e.g., Dixon et al., 2015) and crab megalopae (Miller et al., 2016). Finally, CO<sub>2</sub> concentrations in excess can cause hypercapnia (excess CO<sub>2</sub> in blood) in organisms (Mintenbeck et al., 2012; Macek et al., 2016; Pimentel et al., 2016; Feely et al., 2018; Davenport, 2019). Each of these carbonate system variables can cause stress for marine organisms and may be compounded by concurrent stressor combinations (Kroeker et al., 2017) of temperature, salinity, and dietary availability.

Considerable research has provided insight into how organisms from the GOM respond to OA (Tables S1 and S2), but there are still critical gaps for key environmental components, such as carbonate chemistry data at the sediment–water interface where commercial species like lobster, sea scallops, and surfclams live. Current bottom water measurements, which are meters above where the organisms reside, suggest that  $\Omega_a$  is below critical levels for marine organisms living there. Although water quality does not likely improve closer to the seafloor, measurements at the sediment/water interface would provide data needed to understand the environment where benthic organisms spend the majority of their lives and reduce uncertainty in our projections. In this study, the seasonal variability and spatial differences of  $\Omega_a$  suggest that the northern reaches (i.e., Scotian Shelf) and near-shore GOM will cross critical biological thresholds 10–20 years before the southern GOM (i.e., Georges Bank) due to the warming in the region (**Figure 9**). Experiments on spatial and seasonal impacts on marine organisms at multiple life stages are limited and require the synergy of chemical and physical oceanography with biological responses. Nearshore regions are common nursery grounds for both vertebrate

and invertebrate marine species (Stevenson et al., 2014; Goode et al., 2019) but are poorly represented in our models. Subsequent projections for such critical habitats and inclusions of new studies on key regional economic species, including the understudied Jonah crab and goosefish, are needed to fully assess vulnerabilities and promote adaptive management plans.

## Conclusions

Dependency of coastal communities on shellfish fisheries resources has increased over the past decade in the GOM, which necessitates understanding the dynamics governing the current and future trends for OA in the region. Many of these commercial resources are considered vulnerable to OA. An increase in biological sensitivity and impact studies, summarized in Tables S1 and S2 in this work, has considerably improved the understanding of potential responses of marine species to OA in combination with other climate stressors like temperature in the GOM, particularly for bivalves. Such efforts still only represent a small fraction of knowledge needed on commercially important species and scarcely address complex interactions through food webs and integrated risks of life stages through different habitats. Although surface OA trends historically have been masked by recent warming and increases in inputs from the Gulf Stream,  $\Omega_a$  below suboptimal thresholds for marine organisms ( $\Omega_a < 1.5$ ) have already been observed in areas of high freshwater influence and subsurface zones.

The combination of regional projections detailed here indicates that  $\Omega_a$  is projected to decline everywhere in the GOM by 2050 under RCP 8.5 with most pronounced impacts in locations near the coast, subsurface, and those associated with freshening. By 2050, the entire GOM will experience suboptimal conditions of aragonite saturation state ( $\Omega_a < 1.5$ ) for most of the year under RCP 8.5. Models with the most pronounced warming experienced the weakest decline in  $\Omega_a$  as a consequence of the compensatory effects of largely warming and lesser salinity changes. Achieving reduced uncertainty of the regional warming trends in the future is a high priority to reduce uncertainty in OA projections for the GOM as well. Despite continued masking of the OA signal into the future, projections still indicate increased duration and intensity of suboptimal conditions for marine organisms for  $\Omega_a$  throughout the GOM under RCP 8.5. These projections are more severe than the global projections for the same domain, emissions scenario, and time horizon but are providing downscaled regional projections. Our projections provide important spatial information for decision making in fisheries and future planning; for example, the Georges Bank is a region that remains above the threshold for the longest period. The Scotian Shelf is one of the regions that experiences the earliest sensitivity threshold, both the surface and the bottom. Future work needs to focus on a better understanding of the influence of variability in the Labrador Current, as well as potential biogeochemical feedbacks (i.e., freshwater alterations and sediment–water interactions) and

potential adaptation strategies for land–ocean management for the nearshore regions.

## Data accessibility statement

Data in **Figure 1** from the University of New Hampshire (UNH) Coastal Marine Laboratory are archived with the Northeast Regional Association of Coastal Ocean Observing Systems (<http://www.neracoo.org/erddap/index.html>). UNH/Pacific Marine Environmental Laboratory CO<sub>2</sub> buoy data shown in **Figure 1** are archived at the National Center for Environmental Information ([https://www.nodc.noaa.gov/ocads/oceans/Coastal/unh\\_ts.html](https://www.nodc.noaa.gov/ocads/oceans/Coastal/unh_ts.html)). UNH total alkalinity and dissolved inorganic carbon data used in the construction of **Figure 4** are archived by the UNH Ocean Process Analysis Laboratory (<https://eos.unh.edu/ocean-process-analysis-laboratory/data>). WHOI data in **Figure 4** are archived by the Biological & Chemical Oceanography Data Management Office (<https://www.bco-dmo.org/project/472577>). GOMECC-1 data used in **Figure 4** are archived by NOAA Atlantic Oceanographic and Meteorological Laboratory (<https://www.aoml.noaa.gov/ocd/gcc/GOMECC1/data.php>); those from GOMECC-2 are archived at National Centers for Environmental Information (NCEI; <https://www.nodc.noaa.gov/oads/data/0117971.xml>, NCEI Accession Number 0117971); those from ECOA-1 are archived at NCEI (<https://www.nodc.noaa.gov/oads/data/0159428.xml>, NCEI Accession number 0159428). Decadal commercial landing statistics for New England fisheries species as reported from the National Oceanic Atmospheric Administration Fisheries Service (2020, [www.st.nmfs.noaa.gov/](http://www.st.nmfs.noaa.gov/)). Output from the three Regional Ocean Modeling System physical simulations used for the projections as well as the control run is provided on a website (<https://www.psl.noaa.gov/ipcc/roms/>) and described further in Alexander et al. (2020).

## Supplemental files

The supplemental material provided as a Microsoft Word document (DOCX) contains additional model evaluation, model metrics, and control/base maps used to generate anomalies in the text. Finally, two supplemental tables are also included which detail the extensive review of the literature on species sensitivities in the region to OA as an update to the table in Gledhill et al. (2015).

**Figure S1.** Increasing importance of shellfish to New England fisheries in terms of total landed value.

**Figure S2.** Trends at WB7 for temperature and salinity.

**Figure S3.** Model evaluation at Coastal Marine Lab and Buoy D for  $\Omega_a$ .

**Figure S4.** Model acidification annual metrics at Buoy D.

**Figure S5.** Total alkalinity ( $\mu\text{mol kg}^{-1}$ ) seasonal CTRL for the Regional Ocean Modeling System model with empirical biogeochemistry.

**Figure S6.** Dissolved inorganic carbon ( $\mu\text{mol kg}^{-1}$ ) seasonal CTRL for the Regional Ocean Modeling System model with empirical biogeochemistry.

**Table S1.** Responses of six commercially important species of the Gulf of Maine to increased ocean acidification conditions.

**Table S2.** Studies on organismal response of species from the Gulf of Maine to ocean acidification conditions.

**Table S3.** Gulf of Maine regional ocean acidification observing capacity description of observations plotted in **Figure 2**.

### Acknowledgments

We would like to acknowledge Shani Rousseau for the extraction of the GSBM model data and for the generation of **Figures 6–8** and David Brickman for fruitful discussions. We would also like to thank the constructive contributions of guest editor Stephenson and our two reviewers: Helen Gurney-Smith and one anonymous reviewer, for their help in improving this article. The views expressed in this article are those of the authors and do not necessarily represent the views or policies of the U.S. Environmental Protection Agency. Any mention of trade names, products, or services does not imply an endorsement by the U.S. government or the U.S. Environmental Protection Agency (EPA). The EPA does not endorse any commercial products, services, or enterprises.

### Funding

SAS and KM acknowledge support from the NOAA Ocean Acidification Program grant NA19OAR0170351, the National Center for Atmospheric Research, which is a major facility sponsored by the National Science Foundation (NSF) under Cooperative Agreement No. 1852977 which supports the Early Career Innovators program.

CWH, JS, and DV support comes from NOAA grants NA15NOS0120155 and NA16NOS0120023. DV support also comes from NASA grant NNX17AK08G. JS also received support from NSF grant C01658377.

KA and DL acknowledge support from the DFO's ACCASP-Ocean Chemistry.

MAA acknowledges support from grants by the NOAA Coastal and Climate Applications (COCA) program NA-15OAR4310133 and NA-17OAR4310268. Support for this work was also provided by the NOAA Integrated Ecosystem Assessment Program.

ZAW acknowledges funding support provided by the Coastal Ocean Institute at Woods Hole Oceanographic Institution, National Science Foundation (OCE-1316040), the Pickman Foundation, and the Tom Haas Fund at the New Hampshire Charitable Foundation.

IM acknowledges the support from the U.S. Environmental Protection Agency Region 1's Water Division in supporting her role on this work.

CB acknowledges funding support provided by the MIT Sea Grant award NA18OAR4170105.

### Competing interests

The authors have declared that no competing interests exist.

### Author contributions

Contributed to conception and design: SAS, JS, DKG, RM.

Contributed to acquisition of data: SAS, JS, DKG, CB, SM, KM, CWH, MA, DL, ZAW, JS, IM, DV.

Contributed to analysis and interpretation of data: SAS, JS, DKG, CB, SM, KM, CWH, MA, DL, ZAW, JS, IM.

Drafted and/or revised the article: SAS, JS, DKG, CB, SM, KM, CWH, MA, DL, ZAW, JS, IM, KA, CL, CM, MW, AP, DV, RM.

Approved the submitted version for publication: SAS, JS, DKG, CB, SM, KM, CWH, MA, DL, ZAW, JS, IM, KA, CL, CM, MW, AP, DV, RM.

### References

- Alexander, MA, Shin, S, Scott, JD, Curchitser, E, Stock, C.** 2020. The response of the northwest Atlantic Ocean to climate change. *Journal of Climate* **33**(2): 405–428. DOI: <https://doi.org/10.1175/JCLI-D-19-0117.1>.
- Bakker, DCE, Pfeil, B, Landa, CS, Metzl, N, O'Brien, KM, Olsen, A, Smith, K, Cosca, C, Harasawa, S, Jones, SD, Nakaoka, S, Nojiri, Y, Schuster, U, Steinhoff, T, Sweeney, C, Takahashi, T, Tilbrook, B, Wada, C, Wanninkhof, R, Alin, SR, Balestrini, CF, Barbero, L, Bates, NR, Bianchi, AA, Bonou, F, Boutin, J, Bozec, Y, Burger, EF, Cai, W-J, Castle, RD, Chen, L, Chierici, M, Currie, K, Evans, W, Featherstone, C, Feely, RA, Fransson, A, Goyet, C, Greenwood, N, Gregor, L, Hankin, S, Hardman-Mountford, NJ, Harlay, J, Hauck, J, Hoppema, M, Humphreys, MP, Hunt, CW, Huss, B, Ibáñez, JSP, Johannessen, T, Keeling, R, Kitidis, V, Körtzinger, A, Kozyr, A, Krasakopoulou, E, Kuwata, A, Landschützer, P, Lauvset, SK, Lefèvre, N, Lo Monaco, C, Manke, A, Mathis, JT, Merlivat, L, Millero, FJ, Monteiro, PMS, Munro, DR, Murata, A, Newberge, T, Omar, AM, Ono, T, Paterson, K, Pearce, D, Pierrot, D, Robbins, LL, Saito, S, Salisbury, S, Schlitzer, R, Schneider, B, Schweitzer, R, Sieger, R, Skjelvan, I, Sullivan, KF, Sutherland, SC, Sutton, AJ, Tadokoro, K, Telszewski, M, Tuma, M, van Heuven, SMAC, Vandemark, D, Ward, B, Watson, AJ, Xu, S.** 2016. A multi-decade record of high-quality  $f\text{CO}_2$  data in version 3 of the Surface Ocean  $\text{CO}_2$  Atlas (SOCAT). *Earth System Science Data* **8**: 383–413. DOI: <https://doi.org/10.5194/essd-8-383-2016>.
- Bates, NR, Astor, YM, Church, MJ, Currie, K, Dore, JE, González-Dávila, M, Lorenzoni, L, Muller-Karger, F, Olafsson, J, Santana-Casiano, JM.** 2014. A time-series view of changing ocean chemistry due to ocean uptake of anthropogenic  $\text{CO}_2$  and ocean acidification. *Oceanography* **27**: 126–141. DOI: <https://doi.org/10.5670/oceanog.2014.16>.
- Boavida-Portugal, J, Rosa, R, Calado, R, Pinto, M, Boavida-Portugal, I, Araújo, MB, Guilhaumon F.** 2018. Climate change impacts on the distribution of coastal lobsters. *Marine Biology* **165**(12): 186. DOI: <https://doi.org/10.1007/s00227-018-3441-9>.
- Bopp, L, Resplandy, L, Orr, JC, Doney, SC, Dunne, JP, Gehlen, M, Halloran, P, Heinze, C, Ilyina, T, Séférian, R, Tjiputra, J, Vichi, M.** 2013. Multiple stressors of ocean ecosystems in the 21st century: Projections with CMIP5 models. *Biogeosciences* **10**:

- 6225–6245. DOI: <https://doi.org/10.5194/bg-10-6225-2013>.
- Brickman, D, Alexander, MA, Pershing, A, Scott, JD, Wang, ZA.** n.d. Projections of physical conditions in the Gulf of Maine in 2050. *Elementa: Science of the Anthropocene*, in press.
- Caldeira, K, Wickett, ME.** 2003. Anthropogenic carbon and ocean pH. *Nature* **425**: 365. DOI: <https://doi.org/10.1038/425365a>.
- Chen, K, Gawarkiewicz, GG, Lentz, SJ, Bane, JM.** 2014. Diagnosing the warming of the Northeastern U.S. Coastal Ocean in 2012: A linkage between the atmospheric jet stream variability and ocean response. *Journal of Geophysical Research: Oceans* **119**: 218–227. DOI: <https://doi.org/10.1002/2013JC009393>.
- Chen, K, Kwon, YO.** 2018. Does Pacific variability influence the Northwest Atlantic shelf temperature? *Journal of Geophysical Research: Oceans* **123**: 4110–4131. DOI: <https://doi.org/10.1029/2017JC013414>.
- Chen, Z, Kwon, YO, Chen, K, Fratantoni, P, Gawarkiewicz, G, Joyce, TM.** 2020. Long-term SST variability on the northwest Atlantic continental shelf and slope. *Geophysical Research Letters* **47**. DOI: <https://doi.org/10.1029/2019GL085455>.
- Claret, M, Galbraith, ED, Palter, JB, Bianchi, D, Fennel, K, Gilbert, D, Dunne, JP.** 2018. Rapid coastal deoxygenation due to ocean circulation shift in the northwest Atlantic. *Nature Climate Change* **8**: 868–872. DOI: <https://doi.org/10.1038/s41558-018-0263-1>.
- Clements, JC, Hunt, HL.** 2017. Effects of CO<sub>2</sub> driven sediment acidification on infaunal marine bivalves: A synthesis. *Marine Pollution Bulletin* **117**(1-2): 6–16. DOI: <https://doi.org/10.1016/j.marpolbul.2017.01.053>.
- Clements, JC, Hunt, HL.** 2018. Testing for sediment acidification effects on within-season variability in juvenile soft-shell clam (*Mya arenaria*) abundance on the northern shore of the Bay of Fundy. *Estuaries and Coasts* **41**(2): 471–483. DOI: <https://doi.org/10.1007/s12237-017-0270-x>.
- Cooley, SR, Doney, SC.** 2009. Anticipating ocean acidification's economic consequences for commercial fisheries. *Environmental Research Letters* **4**(2). DOI: <https://doi.org/10.1088/1748-9326/4/2/024007>.
- Cooley, SR, Rheuban, JE, Hart, DR, Luu, V, Glover, DM, Hare, JA, Doney, SC.** 2015. An integrated assessment model for helping the United States sea scallop (*Placopecten magellanicus*) fishery plan ahead for ocean acidification and warming. *PLoS One* **10**(5): e0124145–e0124145. DOI: <https://doi.org/10.1371/journal.pone.0124145>.
- Davenport, J.** 2019. Fish: Ecophysiology, in Cochran, JK, Bokuniewicz, HJ, Yager, P eds., *Encyclopedia of ocean sciences*. Cork, Ireland. Academic Press: 168–174. DOI: <https://doi.org/10.1016/B978-0-12-409548-9.11185-6>.
- Dickey, G, Preziosi, BM, Clark, CT, Bowden, TJ.** 2018. The impact of ocean acidification on the byssal threads of the blue mussel (*Mytilus edulis*). *PLoS One* **13**(10): e0205908.
- Dickson, AG.** 1990a. Standard potential of the reaction: AgCl(s) + 1/2 H<sub>2</sub>(g) = Ag(s) + HCl(aq), and the standard acidity constant of the ion HSO<sub>4</sub>—In synthetic seawater from 273.15 to 318.15 K. *Journal of Chemical Thermodynamics* **22**: 113–127. DOI: [https://doi.org/10.1016/0021-9614\(90\)90074-Z](https://doi.org/10.1016/0021-9614(90)90074-Z).
- Dickson, AG.** 1990b. Thermodynamics of the dissociation of boric acid in synthetic sea water from 273.15 to 318.15 K. *Deep Sea Research Part A. Oceanographic Research Papers* **37**: 755–766. DOI: [https://doi.org/10.1016/0198-0149\(90\)90004-F](https://doi.org/10.1016/0198-0149(90)90004-F).
- Dixon, DL, Jennings, AR, Atema, J, Munday, PL.** 2015. Odor tracking in sharks is reduced under future ocean acidification conditions. *Global Change Biology* **21**(4): 1454–1462. DOI: <https://doi.org/10.1111/gcb.12678>.
- Dixon, DL, Munday, PL, Jones, GP.** 2010. Ocean acidification disrupts the innate ability of fish to detect predator olfactory cues. *Ecology Letters* **13**(1): 68–75. DOI: <https://doi.org/10.1111/j.1461-0248.2009.01400.x>.
- Doney, SC, Fabry, VJ, Feely, RA, Kleypas, JA.** 2009. Ocean acidification: The other CO<sub>2</sub> problem. *Annual Review of Marine Science* **1**: 169–192. DOI: <https://doi.org/10.1146/annurev.marine.010908.163834>.
- Doney, SC, Mahowald, N, Lima, I, Feely, RA, Mackenzie, FT, Lamarque, JF, Rasch, PJ.** 2007. Impact of anthropogenic atmospheric nitrogen and sulfur deposition on ocean acidification and the inorganic carbon system. *Proceedings of the National Academy of Sciences* **104**(37): 14580–14585. DOI: <https://doi.org/10.1073/pnas.0702218104>.
- Ekstrom, JA, Suatoni, L, Cooley, SR, Pendleton, LH, Waldbusser, GG, Cinner, JE, Ritter, J, Langdon, C, van Hooidonk, R, Gledhill, D, Wellman, K, Beck, MW, Brander, LM, Rittschof, D, Doherty, C, Edwards, PET, Portela, R.** 2015. Vulnerability and adaptation of US shellfisheries to ocean acidification. *Nature Climate Change* **5**: 207–215. DOI: <https://doi.org/10.1038/nclimate2508>.
- Fay, G, Link, JS, Hare, JA.** 2017. Assessing the effects of ocean acidification in the Northeast US using an end-to-end marine ecosystem model. *Ecological Modelling* **347**: 1–10. DOI: <https://doi.org/10.1016/j.ecolmodel.2016.12.016>.
- Feely, RA, Doney, SC, Cooley, SR. 2009. Ocean acidification: Present conditions and future changes in a high-CO<sub>2</sub> world. *Oceanography* **22**(4): 36–47. DOI: <https://doi.org/10.5670/oceanog.2009.95>.
- Feely, RA, Okazaki, RR, Cai, WJ, Bednaršek, N, Alin, SR, Byrne, RH, Fassbender, A.** 2018. The combined effects of acidification and hypoxia on pH and aragonite saturation in the coastal waters of the California current ecosystem and the northern Gulf of Mexico. *Continental Shelf Research* **152**: 50–60. DOI: <https://doi.org/10.1016/j.csr.2017.11.002>.
- Feely, RA, Sabine, CL, Hernandez-Ayon, JM, Ianson, D, Hales, B.** 2008. Evidence for upwelling of corrosive

- “acidified” water onto the continental shelf. *Science* **320**(5882): 1490–1492. DOI: <https://doi.org/10.1126/science.1155676>.
- Fennel, K, Wilkin, J, Previdi, M, Najjar, R.** 2008. Denitrification effects on air-sea CO<sub>2</sub> flux in the coastal ocean: Simulations for the northwest North Atlantic. *Geophysical Research Letters* **35**(24). DOI: <https://doi.org/10.1029/2008GL036147>.
- Friedlingstein, P, Jones, MW, O’Sullivan, M, Andrew, RM, Hauck, J, Peters, GP, Peters, W, Pongratz, J, Sitch, S, Le Quéré, C, Bakker, DCE, Canadell, JG, Ciais, P, Jackson, RB, Anthoni, P, Barbero, L, Bastos, A, Bastrikov, V, Becker, M, Bopp, L, Buitenhuis, E, Chandra, N, Chevallier, F, Chini, LP, Currie, KI, Feely, RA, Gehlen, M, Gilfillan, D, Gkritzalis, T, Goll, DS, Gruber, N, Gutekunst, S, Harris, I, Haverd, V, Houghton, RA, Hurtt, G, Ilyina, T, Jain, AK, Joetzier, E, Kaplan, JO, Kato, E, Klein Goldewijk, K, Korsbakken, JI, Landschützer, P, Lauvset, SK, Lefèvre, N, Lenton, A, Lienert, S, Lombardozzi, D, Marland, G, McGuire, PC, Melton, JR, Metzl, N, Munro, DR, Nabel, JEMS, Nakaoka, SI, Neill, C, Omar, AM, Ono, T, Peregon, A, Pierrot, D, Poulter, B, Rehder, G, Resplandy, L, Robertson, E, Rödenbeck, C, Séférian, R, Schwinger, J, Smith, N, Tans, PP, Tian, H, Tilbrook, B, Tubiello, FN, van der Werf, GR, Wiltshire, AJ, Zaehle, S.** 2019. Global Carbon Budget 2019. *Earth System Science Data* **11**: 1783–1838. DOI: <https://doi.org/10.5194/essd-11-1783-2019>.
- Gattuso, JP, Magnan, A, Billé, R, Cheung, WWL, Howes, EL, Joos, F, Allemand, D, Bopp, L, Cooley, SR, Eakin, CM, Hoegh-Guldberg, O, Kelly, RP, Pörtner, H-O, Rogers, AD, Baxter, JM, Laffoley, D, Osborn, D, Rankovic, A, Rochette, J, Sumaila, UR, Treyer, S, Turley, C.** 2015. Contrasting futures for ocean and society from different anthropogenic CO<sub>2</sub> emissions scenarios. *Science* **349**(6243): aac4722. DOI: <https://doi.org/10.1126/science.aac4722>.
- Gazeau, F, Parker, LM, Comeau, S, Gattuso, JP, O’Connor, WA, Martin, S, Pörtner, H-O, Ross, PM.** 2013. Impacts of ocean acidification on marine shelled molluscs. *Marine Biology* **160**(8): 2207–2245. DOI: <https://doi.org/10.1007/s00227-013-2219-3>.
- Gehlen, M, Barciela, R, Bertino, L, Brasseur, P, Butenschön, M, Chai, F, Crise, A, Drillet, Y, Ford, D, Lavoie, D, Lehodey, P, Perruche, C, Samuelsen, A.** 2015. Building the capacity for forecasting marine biogeochemistry and lower tropic level ecosystems: Recent advances and future developments. *Journal of Operational Oceanography* **8**(Sup1): s168–s187.
- Geyer, WR, Signell, RP, Fong, DA, Wang, J, Anderson, DM, Keafer, BA.** 2004. The freshwater transport and dynamics of the western Maine coastal current. *Continental Shelf Research* **24**(12): 1339–1357. DOI: <https://doi.org/10.1016/j.csr.2004.04.001>.
- Gledhill, DK, White, MM, Salisbury, J, Thomas, H, Mlsna, I, Liebman, M, Mook, B, Grear, J, Candelmo, AC, Chambers, RC, Gobler, CJ, Hunt, CW, King, AL, Price, NN, Signorini, SR, Stancioff, E, Stymiest, C, Wahle, RA, Waller, JD, Rebuck, ND, Wang, ZA, Capson, TL, Morrison, JR, Cooley, SR, Doney, SC.** 2015. Ocean and coastal acidification off New England and Nova Scotia. *Oceanography* **28**(2):182–197. DOI: <http://dx.doi.org/10.5670/oceanog.2015.41>.
- Goode, A, Brady, DC, Steneck, R, Wahle, R.** 2019. The brighter side of climate change: Ocean warming crosses a biological threshold to amplify an iconic fishery. *Global Change Biology* **25**: 3906–3917. DOI: <https://doi.org/10.1111/gcb.14778>.
- Griffith, AW, Gobler, CJ.** 2017. Transgenerational exposure of North Atlantic bivalves to ocean acidification renders offspring more vulnerable to low pH and additional stressors. *Scientific Reports* **7**(1): 11394. DOI: <https://doi.org/10.1038/s41598-017-11442-3>.
- Grodsky, SA, Reul, N, Chapron, B, Carton, JA, Bryan, FO.** 2017. Interannual surface salinity on Northwest Atlantic shelf. *Journal of Geophysical Research: Oceans* **122**: 3638–3659. DOI: <https://doi.org/10.1002/2016JC012580>.
- Hare, JA, Morrison, WE, Nelson, MW, Stachura, MM, Teeters, EJ, Griffis, RB, Alexander, MA, Scott, JD, Alade, L, Bell, RJ, Chute, AS, Curti, KL, Curtis, TH, Kircheis, D, Kocik, JF, Lucey, SM, McCandless, CT, Milke, LM, Richardson, DE, Robillard, E, Walsh, HJ, McManus, MC, Marancik, KE, Griswold, CA.** 2016. A vulnerability assessment of fish and invertebrates to climate change on the Northeast U.S. Continental Shelf. *PLoS One* **11**(2): e0146756. DOI: <https://doi.org/10.1371/journal.pone.0146756>.
- Harrington AM, Hamlin HJ.** 2019. Ocean acidification alters thermal cardiac performance, hemocyte abundance, and hemolymph chemistry in subadult American lobsters *Homarus americanus* H. Milne Edwards, 1837 (Decapoda: Malacostraca: Nephropidae). *Journal of Crustacean Biology* **39**(4): 468–476. DOI: <https://doi.org/10.1093/jcobiol/ruz015>.
- Hunt, CW, Salisbury, JE, Vandemark, D, McGillis, W.** 2011. Contrasting carbon dioxide inputs and exchange in three adjacent New England estuaries. *Estuaries and Coasts* **34**: 68–77. DOI: <https://doi.org/10.1007/s12237-010-9299-9>.
- Hunt, CW, Snyder, L, Salisbury, JE, Vandemark, D, McDowell, WH.** 2017. SIPCO2: A simple, inexpensive surface water pCO<sub>2</sub> sensor. *Limnology and Oceanography: Methods* **15**: 291–301. DOI: <https://doi.org/10.1002/lom3.10157>.
- Jaini, M, Wahle, RA, Thomas, AC, Weatherbee, R.** 2018. Spatial surface temperature correlates of American lobster (*Homarus americanus*) settlement in the Gulf of Maine and southern New England shelf. *Bulletin of Marine Science* **94**(3): 737–751. DOI: <https://doi.org/10.5343/bms.2017.1141>.



- Jiang, L, Carter, BR, Feely, RA, Lauvset, SK, Olsen, A.** 2019. Surface ocean pH and buffer capacity: Past, present and future. *Scientific Reports* **9**: 18624. DOI: <https://doi.org/10.1038/s41598-019-55039-4>.
- Jin, P, Wang, T, Liu, N, Dupont, S, Beardall, J, Boyd, PW, Riebesell, Gao, K.** 2015. Ocean acidification increases the accumulation of toxic phenolic compounds across trophic levels. *Nature Communications* **6**(1): 8714. DOI: <https://doi.org/10.1038/ncomms9714>.
- Kang, D, Curchitser, EN.** 2013. Gulf Stream eddy characteristics in a high-resolution ocean model. *Journal of Geophysical Research: Oceans* **118**: 4474–4487. DOI: <https://doi.org/10.1002/jgrc.20318>.
- Keppel, EA, Scrosati, RA, Courtenay, SC.** 2012. Ocean acidification decreases growth and development in American lobster (*Homarus americanus*) larvae. *Journal of Northwest Atlantic Fishery Science* **44**: 61–66. DOI: <https://doi.org/10.2960/J.v44.m683>.
- Kroeker, KJ, Kordas, RL, Harley, CDG.** 2017. Embracing interactions in ocean acidification research: Confronting multiple stressor scenarios and context dependence. *Biology Letters* **13**. DOI: <https://doi.org/10.1098/rsbl.2016.0802>.
- Kwiatkowski, L, Orr, J.** 2018. Diverging seasonal extremes for ocean acidification during the twenty-first century. *Nature Climate Change* **8**: 141–145. DOI: <https://doi.org/10.1038/s41558-017-0054-0>.
- Lavoie, D, Lambert, N, Gilbert, D.** 2019. Projections of future trends in biogeochemical conditions in the Northwest Atlantic using CMIP5 Earth System Models. *Atmosphere-Ocean* **57**(1): 18–40.
- Lavoie, D, Lambert, N, Rousseau, S, Dumas, J, Chassé, J, Long, Z, Perrie, W, Starr, M, Brickman, D, Azetsu-Scott, K.** 2020. Projections of future biochemical conditions in the Gulf of St. Lawrence, on the Scotian Shelf and in the Gulf of Maine using a regional climate model. *Canadian Technical Report of Hydrography and Ocean Sciences* **334**: xiii + 102. Available at <http://www.publications.gc.ca/site/eng/9.892092/publication.html>.
- Leo, E, Dahlke, FT, Storch, D, Pörtner, H-O, Mark, FC.** 2018. Impact of ocean acidification and warming on the bioenergetics of developing eggs of Atlantic herring *Clupea harengus*. *Conservation Physiology* **6**(1). Oxford Academic. DOI: <https://doi.org/10.1093/conphys/coy050>.
- Le Quéré, C, Andrew, RM, Friedlingstein, P, Sitch, S, Pongratz, J, Manning, AC, Korsbakken, JI, Peters, GP, Canadell, JG, Jackson, RB, Boden, TA, Tans, PP, Andrews, OD, Arora, VK, Bakker, DCE, Barbero, L, Becker, M, Betts, RA, Bopp, L, Chevallier, F, Chini, LP, Ciais, P, Cosca, CE, Cross, J, Currie, K, Gasser, T, Harris, I, Hauck, J, Haverd, V, Houghton, RA, Hunt, CW, Hurtt, G, Ilyina, T, Jain, AK, Kato, E, Kautz, M, Keeling, RF, Golde-wijk, KK, Körtzinger, A, Landschützer, P, Lefèvre, N, Lenton, A, Lienert, S, Lima, I, Lombardozzi, D, Metzl, N, Millero, F, Monteiro, PMS, Munro, DR, Nabel, JEMS, Nakaoka, S, Nojiri, Y, Padin, XA, Peregón, A, Pfeil, B, Pierrot, D, Poulter, B, Rehder, G, Reimer, J, Rödenbeck, C, Schwinger, J, Séférian, R, Skjelvan, I, Stocker, BD, Tian, H, Tilbrook, B, Tubiello, FN, van der Laan-Luijckx, IT, van der Werf, GR, van Heuven, S, Viovy, N, Vuichard, N, Walker, AP, Watson, AJ, Wiltshire, AJ, Zaehle, A, Zhu, D.** 2018. Global Carbon Budget 2017. *Earth System Science Data* **10**(1): 405–448. DOI: <https://doi.org/10.5194/essd-10-405-2018>.
- Lewis, E, Wallace, DWR. 1998. *Program developed for CO<sub>2</sub> system calculations. ORNL/CDIAC-105*. Carbon Dioxide Information Analysis Center, Oak Ridge National Laboratory, U.S. Department of Energy, Oak Ridge, Tennessee. DOI: [https://doi.org/10.3334/CDIAC/otg.CO2SYS\\_DOS\\_CDIAC\\_105](https://doi.org/10.3334/CDIAC/otg.CO2SYS_DOS_CDIAC_105).
- Long, WC, Swiney, KM, Foy, RJ.** 2016a. Effects of high pCO<sub>2</sub> on Tanner crab reproduction and early life history, Part II: Carryover effects on larvae from oogenesis and embryogenesis are stronger than direct effects. *ICES Journal of Marine Science* **73**(3): 836–848. DOI: <https://doi.org/10.1093/icesjms/fsv251>.
- Long, ZX, Perrie, W, Chasse, J, Brickman, D, Guo, LL, Drozdowski, A, Hu, HB.** 2016b. Impacts of climate change in the Gulf of St. Lawrence. *Atmosphere-Ocean* **54**(3): 337–351. DOI: <https://doi.org/10.1080/07055900.2015.1029869>.
- Maček, I, Vodnik, D, Pfanz, H, Low-Décarie, E, Dumbrell, AJ.** 2016. Chapter six, Locally extreme environments as natural long-term experiments in ecology, in Dumbrell, AJ, Kordas, RL, Woodward, G eds., *Large-scale ecology: Model systems to global perspectives* (Vol. 55): 283–323. DOI: <https://doi.org/10.1016/bs.aecr.2016.08.001>.
- Maine 126th Legislature, 2nd Session. 2015. Final report of the commission to study the effects of coastal and ocean acidification and its existing and potential effects on species that are commercially harvested and grown along the Maine coast. Maine Department of Marine Resources.** 2019. Maine Aquaculture Harvest Data. Available at <https://www.maine.gov/dmr/aquaculture/harvestdata/index.html>. Accessed 7 October 2019.
- McGarry, K, Siedlecki, SA, Salisbury, J, Alin, SR.** 2021. Multiple linear regression models for reconstructing and exploring processes controlling the carbonate system of the northeast US from basic hydrographic data. *Journal of Geophysical Research: Oceans* **126**. DOI: <https://doi.org/10.1029/2020JC016480>.
- McLean, EL, Katenka, NV, Seibel, BA.** 2018. Decreased growth and increased shell disease in early benthic phase *Homarus americanus* in response to elevated CO<sub>2</sub>. *Marine Ecology Progress Series* **596**: 113–126. DOI: <https://doi.org/10.3354/meps12586>.
- Menu-Courey, K, Noisette, F, Piedalue, S, Daoud, D, Blair, T, Blier, PU, Azetsu-Scott, K, Calosi, P.** 2019. Energy metabolism and survival of the juvenile recruits of the American lobster (*Homarus americanus*) exposed to a gradient of elevated seawater pCO<sub>2</sub>. *Marine Environmental Research* **143**: 111–

123. DOI: <https://doi.org/10.1016/j.marenvres.2018.10.002>.
- Meseck, SL, Mercaldo-Allen, R, Clark, P, Kuropat, C, Redman, D, Veilleux, D, Milke, L.** n.d. Ocean acidification effects on larval Atlantic surfclams from Long Island Sound, Connecticut, USA. *Fisheries Bulletin*, in press.
- Meseck, SL, Mercaldo-Allen, R, Kuropat, C, Clark, P, Goldberg, R.** 2018. Variability in sediment-water carbonate chemistry and bivalve abundance after bivalve settlement in Long Island Sound, Milford, Connecticut. *Marine Pollution Bulletin* **135**: 165–175. DOI: <https://doi.org/10.1016/j.marpolbul.2018.07.025>.
- Miller, CA, Waldbusser, GG.** 2016. A post-larval stage-based model of hard clam *Mercenaria mercenaria* development in response to multiple stressors: Temperature and acidification severity. *Marine Ecology Progress Series* **558**, 35–49. DOI: <https://doi.org/10.3354/meps11882>.
- Millero, FJ.** 2010. Carbonate constants for estuarine waters. *Marine and Freshwater Research* **61**: 139–142. DOI: <https://doi.org/doi:10.1071/MF09254>.
- Mintenbeck, K, Barrera-Oro, ER, Brey, T, Jacob, U, Knust, R, Mark, FC, Moreira, E, Strobel, A, Arntz, EW.** 2012. Impact of climate change on fishes in complex Antarctic food webs, in Jacob, U, Woodward, G eds., *Global change in multispecies systems: Part I* (Vol. **46**): 351–426. DOI: <https://doi.org/10.1016/B978-0-12-396992-7.00006-X>.
- Mountain, DG.** 2012. Labrador slope water entering the Gulf of Maine—Response to the North Atlantic Oscillation. *Continental Shelf Research* **47**: 150–155. DOI: <https://doi.org/10.1016/j.csr.2012.07.008>.
- Narita, D, Rehdanz, K, Tol, RSJ.** 2012. Economic costs of ocean acidification: A look into the impacts on global shellfish production. *Climatic Change* **113**(3): 1049–1063. DOI: <https://doi.org/10.1007/s10584-011-0383-3>.
- NOAA Fisheries.** 2019. Annual commercial landings statistics. Available at <https://foss.nmfs.noaa.gov/apexfoss/f?p=215:200:10897789256554::NO::>. Accessed 15 May 2020
- Oppenheim, N, Wahle, R, Brady, DC, Goode, A, Pershing, A.** 2019. Forecasting fishery trends in a warming ocean: A modeling framework using early life stages of the American lobster. *Ecological Applications* **29**(8): e02006. DOI: <https://doi.org/10.1002/eap.2006>.
- Orr, JC, Fabry, VJ, Aumont, O, Bopp, L, Doney, SC, Feely, RA, Gnanadesikan, A, Gruber, N, Ishida, A, Joos, F, Key, RM, Lindsay, K, Maier-Reimer, E, Matear, R, Monfray, P, Mouchet, A, Najjar, RG, Plattner, G-K, Rodgers, KB, Sabine, CL, Sarmiento, JL, Slater, RD, Totterdell, IJ, Weirig, M-F, Yamanaka, Y, Yool, A.** 2005. Anthropogenic ocean acidification over the twenty-first century and its impact on calcifying organisms. *Nature* **437**: 681. DOI: <https://doi.org/10.1038/nature04095>.
- Pershing, AJ, Alexander, MA, Hernandez, CM, Kerr, LA, Le Bris, A, Mills, KE, Nye, JA, Record, NR, Scannell, HA, Scott, JD, Sherwood, GD, Thomas, AC.** 2015. Slow adaptation in the face of rapid warming leads to collapse of the Gulf of Maine cod fishery. *Science* **350**(6262): 809–812. DOI: <https://doi.org/10.1126/science.aac9819>.
- Pettigrew, NR, Churchill, JH, Janzen, CD, Mangum, LJ, Signell, RP, Thomas, AC, Townsend, DW, Wallinga, JP, Xue, H.** 2005. The kinematic and hydrographic structure of the Gulf of Maine Coastal Current. *Deep Sea Research Part II: Topical Studies in Oceanography* **52**(19): 2369–2391. DOI: <https://doi.org/10.1016/j.dsr2.2005.06.033>.
- Pilcher, DJ, Siedlecki, SA, Hermann, AJ, Coyle, KO, Mathis, JT, Evans, W.** 2018. Simulated impact of glacial runoff on CO<sub>2</sub> uptake in the Gulf of Alaska. *Geophysical Research Letters* **45**(2). DOI: <https://doi.org/10.1002/2017GL075910>.
- Pimentel, MS, Faleiro, F, Marques, T, Bispo, R, Dionisio, G, Faria, AM, Machado, J, Peck, MA, Portner, H, Pousao-Ferreira, P, Goncalves, EJ, Rosa, R.** 2016. Foraging behaviour, swimming performance and malformations of early stages of commercially important fishes under ocean acidification and warming. *Climatic Change* **137**: 495–509. DOI: <https://doi.org/10.1007/s10584-016-1682-5>.
- Pousse, E, Poach, ME, Redman, DH, Sennfelder, G, White, LE, Lindsey, JM, Munroe, D, Hart, D, Hennen, D, Dixon, MS, Li, Y, Wikfors, GH, Meseck, SL.** 2020. Energetic response of Atlantic surfclam *Spisula solidissima* to ocean acidification. *Marine Pollution Bulletin* **161**: 111740.
- Pringle, JM.** 2006. Sources of variability in Gulf of Maine circulation, and the observations needed to model it. *Deep Sea Research Part II: Topical Studies in Oceanography* **53**(23): 2457–2476. DOI: <https://doi.org/10.1016/j.dsr2.2006.08.015>.
- Qi, D, Chen, L, Chen, B, Gao, Z, Zhong, W, Feely, RA, Anderson, LG, Sun, H, Chen, J, Chen, M, Zhan, L, Zhang, Y, Cai, W-J.** 2017. Increase in acidifying water in the western Arctic Ocean. *Nature Climate Change* **7**: 195. DOI: <https://doi.org/10.1038/nclimate3228>.
- Raven, JA, Gobler, CJ, Hansen, PJ.** 2020. Dynamic CO<sub>2</sub> and pH levels in coastal, estuarine, and inland waters: Theoretical and observed effects on harmful algal blooms. *Harmful Algae* **91**: 101594. DOI: <https://doi.org/10.1016/j.hal.2019.03.012>.
- Rheuban, JE, Doney, SC, Cooley, SR, Hart, DR.** 2018. Projected impacts of future climate change, ocean acidification, and management on the US Atlantic sea scallop (*Placopecten magellanicus*) fishery. *PLoS One* **13**(9): e0203536. DOI: <https://doi.org/10.1371/journal.pone.0203536>.
- Rheuban, JE, Doney, SC, McCorkle, DC, Jakuba, RW.** 2019. Quantifying the effects of nutrient enrichment and freshwater mixing on coastal ocean acidification. *Journal of Geophysical Research: Oceans*

- 124: 9085–9100. DOI: <https://doi.org/10.1029/2019JC015556>.
- Rheuban, JE, Gassett, PR, McCorkle, DC, Hunt, CW, Liebman, M, Bastidas, C, O'Brien-Clayton, K, Pimenta, AR, Silva, E, Vlahos, P, Woosley, RJ, Ries, J, Liberti, CM, Grear, J, Salisbury, J, Brady, DC, Guay, K, LaVigne, M, Strong, AL, Stancioff, E, Turner, E.** 2021. Synoptic assessment of coastal total alkalinity through community science. *Environmental Research Letters* **16**(2): 024009.
- Rheuban, JE, Kavanaugh, MT, Doney, SC.** 2017. Implications of future Northwest Atlantic bottom temperatures on the American lobster (*Homarus americanus*) fishery. *Journal of Geophysical Research: Oceans* **122**(12): 9387–9398. DOI: <https://doi.org/10.1002/2017JC012949>.
- Richaud, B, Kwon, Y-O, Joyce, TM, Fratantoni, PS, Lentz, SJ.** 2016. Surface and bottom temperature and salinity climatology along the continental shelf off the Canadian and U.S. East Coasts. *Continental Shelf Research* **124**: 165–181. DOI: <https://doi.org/10.1016/j.csr.2016.06.005>.
- Rodriguez-Dominguez, A, Connell, SD, Baziret, C, Nagelkerken, I.** 2018. Irreversible behavioural impairment of fish starts early: Embryonic exposure to ocean acidification. *Marine Pollution Bulletin* **133**: 562–567. DOI: <https://doi.org/10.1016/j.marpolbul.2018.06.004>.
- Saba, VS, Griffies, SM, Anderson, WG, Winton, M, Alexander, MA, Delworth, TL, Hare, JA, Harrison, MJ, Rosati, A, Vecchi, GA, Zhang, R.** 2016. Enhanced warming of the Northwest Atlantic Ocean under climate change. *Journal of Geophysical Research: Oceans* **121**: 118–132. DOI: <https://doi.org/10.1002/2015JC011346>.
- Salisbury, JE, Green, M, Hunt, C, Campbell, J.** 2008. Coastal acidification by rivers: A threat to shellfish? *Eos, Transactions American Geophysical Union* **89**: 513. DOI: <https://doi.org/10.1029/2008EO500001>.
- Salisbury, JE, Jönsson, BF.** 2018. Rapid warming and salinity changes in the Gulf of Maine alter surface ocean carbonate parameters and hide ocean acidification. *Biogeochemistry* **141**(3): 401–418. DOI: <https://doi.org/10.1007/s10533-018-0505-3>.
- Schulz, KG, Bach, LT, Bellerby, RG, Bermúdez, R, Büdenbender, J, Boxhammer, T, Czerny, J, Engel, A, Ludwig, A, Meyerhöfer, Larsen, A, Paul, AJ, Sswat, M, Riebesell, U.** 2017. Phytoplankton blooms at increasing levels of atmospheric carbon dioxide: Experimental evidence for negative effects on prymnesiophytes and positive on small picoeukaryotes. *Frontiers in Marine Science* **4**: 64. DOI: <https://doi.org/10.3389/fmars.2017.00064>.
- Shadwick, EH, Thomas, H, Azetsu-Scott, K, Greenan, BJW, Head, E, Horne, E.** 2011. Seasonal variability of dissolved inorganic carbon and surface water pCO<sub>2</sub> in the Scotian Shelf region of the Northwestern Atlantic. *Marine Chemistry* **124**: 23–37. DOI: <https://doi.org/10.1016/j.marchem.2010.11.004>.
- Shchepetkin, AF, McWilliams, JC.** 2005. The Regional Oceanic Modeling System (ROMS): A split-explicit, free-surface, topography-following-coordinate oceanic model. *Ocean Modelling* **9**(4): 347–404. DOI: <https://doi.org/10.1016/j.ocemod.2004.08.002>.
- Siedlecki, SA, Pilcher, DJ, Hermann, AJ, Coyle, K, Mathis, J.** 2017. The importance of freshwater to spatial variability of aragonite saturation state in the Gulf of Alaska. *Journal of Geophysical Research: Oceans* **122**(11). DOI: <https://doi.org/10.1002/2017JC012791>.
- Stevenson, D, Tuxbury, S, Johnson, M, Boelke, C.** 2014. Shallow water benthic habitats in the Gulf of Maine: A summary of habitat use by common fish and shellfish species in the Gulf of Maine greater Atlantic region. Policy Series 14-01. Gloucester, MA: NOAA Fisheries.
- Stiasny, MH, Mittermayer, FH, Göttler, G, Bridges, CR, Falk-Petersen, I-B, Puvanendran, V, Mortensen, A, Reusch, TBH, Clemmesen, C.** 2018. Effects of parental acclimation and energy limitation in response to high CO<sub>2</sub> exposure in Atlantic cod. *Scientific Reports* **8**(1): 8348. DOI: <https://doi.org/10.1038/s41598-018-26711-y>.
- Strong, AL, Kroeker, KJ, Teneva, LT, Mease, LA, Kelly, RP.** 2014. Ocean acidification 2.0: Managing our changing coastal ocean chemistry. *BioScience* **64**(7): 581–592. DOI: <https://doi.org/10.1093/biosci/biu072>.
- Sutton, AJ, Feely, RA, Maenner-Jones, S, Musielwicz, S, Osborne, J, Dietrich, C, Monacci, N, Cross, J, Bott, R, Kozyr, A, Andersson, AJ, Bates, NR, Cai, W-J, Cronin, MF, De Carlo, EH, Hales, B, Howden, SD, Lee, CM, Manzello, DP, McPhaden, MJ, Melendez, M, Mickett, JB, Newton, JA, Noakes, SE, Noh, JH, Olafsdottir, SR, Salisbury, JE, Send, U, Trull, TW, Vandemark, DC, Weller, RA.** 2019. Autonomous seawater pCO<sub>2</sub> and pH time series from 40 surface buoys and the emergence of anthropogenic trends. *Earth System Science Data Discussions* **11**: 421–439. DOI: <https://doi.org/10.5194/essd-11-421-2019>.
- Sutton, AJ, Sabine, CL, Feely, RA, Cai, W-J, Cronin, MF, McPhaden, MJ, Morrell, JM, Newton, JA, Noh, J, Olafsdóttir, SR, Salisbury, JE, Send, U, Vandemark, DC, Weller, RA.** 2016. Using present-day observations to detect when anthropogenic change forces surface ocean carbonate chemistry outside preindustrial bounds. *Biogeosciences* **13**(17): 5065–5083. DOI: <https://doi.org/10.5194/bg-13-5065-2016>.
- Takahashi, T, Sutherland, SC, Wanninkhof, R, Sweeney, C, Feely, RA, Chipman, DW, Hales, B, Friederich, FC, Sabine, C, Watson, A, Bakker, DCE, Schuster, U, Metzl, N, Yoshikawa-Inoue, H, Ishii, M, Midorikawa, T, Nojiri, Y, Körtzinger, A, Steinhoff, T, Hoppema, M, Olafsson, J, Arnarson, TS, Tilbrook, B, Johannessen, T, Olsen, A, Bellerby, R, Wong, CS, Delille, B, Bates, NR, de Barr, HJW.** 2009. Climatological mean and decadal change in

- surface ocean pCO<sub>2</sub>, and net sea–air CO<sub>2</sub> flux over the global oceans. *Deep Sea Research Part II: Topical Studies in Oceanography* **56**: 554–577. DOI: <https://doi.org/doi:10.1016/j.dsr2.2008.12.009>.
- Tanaka, K, Chen, Y.** 2016. Modeling spatiotemporal variability of the bioclimate envelope of *Homarus americanus* in the coastal waters of Maine and New Hampshire. *Fisheries Research* **177**: 137–152. DOI: <https://doi.org/10.1016/j.fishres.2016.01.010>.
- Tester, PA, Litaker, RW, Berdalet, E.** 2020. Climate change and harmful benthic microalgae. *Harmful Algae* **91**: 101655. DOI: <https://doi.org/10.1016/j.hal.2019.101655>.
- Timbs JR, Powell EN, Mann R.** 2019. Changes in the spatial distribution and anatomy of a range shift for the Atlantic surfclam *Spisula solidissima* in the Mid-Atlantic Bight and on Georges Bank. *Marine Ecology Progress Series* **620**: 77–97. DOI: <https://doi.org/10.3354/meps12964>.
- Townsend, DW.** 1991. Influences of oceanographic processes on the biological productivity of the Gulf of Maine. *Reviews in Aquatic Sciences* **5**: 211–230.
- Townsend, DW, Pettigrew, NR, Thomas, MA, Neary, MG, McGillicuddy, DJ, O'Donnell, J.** 2015. Water masses and nutrient sources to the Gulf of Maine. *Journal of Marine Research* **73**: 93–122. DOI: <https://doi.org/10.1357/002224015815848811>.
- Townsend, DW, Rebeck, ND, Thomas, MA, Karp-Boss, L, Gettings, RM.** 2010. A changing nutrient regime in the Gulf of Maine. *Continental Shelf Research* **30**(7): 820–832. DOI: <https://doi.org/10.1016/j.csr.2010.01.019>.
- Townsend, DW, Thomas, MA, McGillicuddy, DJ, Rebeck, NR.** 2014. Nutrients and water masses in the Gulf of Maine–Georges Bank region: Variability and importance to blooms of the toxic dinoflagellate *Alexandrium fundyense*. *Deep-Sea Research Part II* **103**: 238–263. DOI: <https://doi.org/10.1016/j.dsr2.2013.08.003>.
- Uppstrom, LR.** 1974. The boron/chlorinity ratio of deep-sea water from the Pacific Ocean. *Deep-Sea Research and Oceanographic Abstracts* **21**(2): 161–162. DOI: [https://doi.org/10.1016/0011-7471\(74\)90074-6](https://doi.org/10.1016/0011-7471(74)90074-6).
- Vandemark, D, Salisbury, JE, Hunt, CW, Shellito, SM, Irish, JD, McGillis, WR, Sabine, CL, Maenner, SM.** 2011. Temporal and spatial dynamics of CO<sub>2</sub> air-sea flux in the Gulf of Maine. *Journal of Geophysical Research: Oceans* **116**: C01012. DOI: <https://doi.org/10.1029/2010JC006408>.
- van Heuven, S, Pierrot, D, Rae, JWB, Lewis, E, Wallace, DWR.** 2011. CO<sub>2</sub>SYS v 1.1, MATLAB program developed for CO<sub>2</sub> system calculations. ORNL/CDIAC-105b. ORNL/CDIAC-105b Oak Ridge Natl. Lab. U.S. DoE. Available at [https://doi.org/10.3334/CDIAC/otg.CO2SYS\\_MATLAB\\_v1.1](https://doi.org/10.3334/CDIAC/otg.CO2SYS_MATLAB_v1.1).
- Vehmaa, A, Almén, AK, Brutemark, A, Paul, AJ, Riebesell, U, Furuhausen, S, Engström-Öst, J.** 2016. Ocean acidification challenges copepod phenotypic plasticity. *Biogeosciences* **13**(22): 6171–6182. DOI: <https://doi.org/10.5194/bg-13-6171-2016>.
- Ventura, A, Schulz, S, Dupont, S.** 2016. Maintained larval growth in mussel larvae exposed to acidified under-saturated seawater. *Scientific Reports* **6**(1): 23728. DOI: <https://doi.org/10.1038/srep23728>.
- Waldbusser, GG, Hales, B, Langdon, C, Haley, BA, Schrader, P, Brunner, EL, Gray, MW, Miller CA, Gimenez, I.** 2015. Saturation-state sensitivity of marine bivalve larvae to ocean acidification. *Nature Climate Change* **5**: 273–280. DOI: <https://doi.org/10.1038/nclimate2479>.
- Waldbusser, GG, Salisbury, JE.** 2014. Ocean acidification in the coastal zone from an organism's perspective: Multiple system parameters, frequency domains, and habitats. *Annual Review of Marine Science* **6**(1): 221–247. DOI: <https://doi.org/10.1146/annurev-marine-121211-172238>.
- Wallace, RB, Baumann, H, Grear, JS, Aller, RC, Gobler, CJ.** 2014. Coastal ocean acidification: The other eutrophication problem. *Estuarine, Coastal and Shelf Science* **148**: 1–13. DOI: <https://doi.org/10.1016/j.ecss.2014.05.027>.
- Waller, JD, Wahle, RA, McVeigh, H, Fields, DM.** 2017. Linking rising pCO<sub>2</sub> and temperature to the larval development and physiology of the American lobster (*Homarus americanus*). *ICES Journal of Marine Science* **74**: 1210–1219.
- Wang, ZA, Lawson, GL, Pilskaln, CH, Maas, AE.** 2017. Seasonal controls of aragonite saturation states in the Gulf of Maine. *Journal of Geophysical Research: Oceans* **122**: 372–389. DOI: <https://doi.org/10.1002/2016jc012373>.
- Wang, ZA, Wanninkhof, R, Cai, W-J, Byrne, RH, Hu, XP, Peng, TH, Huang, WJ.** 2013. The marine inorganic carbon system along the Gulf of Mexico and Atlantic coasts of the United States: Insights from a transregional coastal carbon study. *Limnology and Oceanography* **58**: 325–342. DOI: <https://doi.org/10.4319/lo.2013.58.1.0325>.
- Wanninkhof, R, Barbero, L, Byrne, R, Cai, W-J, Huang, W-J, Zhang, J-Z, Baringer, M, Langdon, C.** 2015. Ocean acidification along the Gulf Coast and East Coast of the USA. *Journal Continental Shelf Research* **98**: 54–71.
- Weiss, RF.** 1970. The solubility of nitrogen, oxygen and argon in water and seawater. *Deep Sea Research and Oceanographic Abstracts* **17**(4): 721–735. DOI: [https://doi.org/10.1016/0011-7471\(70\)90037-9](https://doi.org/10.1016/0011-7471(70)90037-9).
- Wilson, TJB, Cooley, SR, Tai, TC, Cheung, WWL, Tyedmers, PH.** 2020. Potential socioeconomic impacts from ocean acidification and climate change effects on Atlantic Canadian fisheries. *PLoS One* **15**(1): e0226544. DOI: <https://doi.org/10.1371/journal.pone.0226544>.
- Young, CS, Gobler, CJ.** 2018. The ability of macroalgae to mitigate the negative effects of ocean acidification on four species of North Atlantic bivalve. *Biogeosciences* **15**(20): 6167–6183. DOI: <https://doi.org/10.5194/bg-15-6167-2018>.

**How to cite this article:** Siedlecki, SA, Salisbury, J, Gledhill, DK, Bastidas, C, Meseck, S, McGarry, K, Hunt, CW, Alexander, M, Lavoie, D, Wang, ZA, Scott, J, Brady, DC, Mlsna, I, Azetsu-Scott, K, Liberti, CM, Melrose, DC, White, MM, Pershing, A, Vandemark, D, Townsend, DW, Chen, C, Mook, W, Morrison, R. 2021. Projecting ocean acidification impacts for the Gulf of Maine to 2050: New tools and expectations. *Elementa: Science of the Anthropocene* 9(1). DOI: <https://doi.org/10.1525/elementa.2020.00062>

**Domain Editor-in-Chief:** Jody W. Deming, University of Washington, Seattle, WA, USA

**Guest Editor:** Robert Stephenson, Fisheries and Oceans Canada Andrews Biological Station, Canada

**Knowledge Domain:** Ocean Science

**Part of an Elementa Special Feature:** Gulf of Maine 2050: Visioning Regional Resilience and Sustainability

**Published:** May 13, 2021    **Accepted:** March 30, 2021    **Submitted:** May 29, 2020

**Copyright:** © 2021 The Author(s). This is an open-access article distributed under the terms of the Creative Commons Attribution 4.0 International License (CC-BY 4.0), which permits unrestricted use, distribution, and reproduction in any medium, provided the original author and source are credited. See <http://creativecommons.org/licenses/by/4.0/>.



*Elem Sci Anth* is a peer-reviewed open access journal published by University of California Press.

OPEN ACCESS The Open Access logo, consisting of the words "OPEN ACCESS" followed by a circular icon containing a stylized 'A'.